VYSOKÉ UČENÍ TECHNICKÉ V BRNĚ

BRNO UNIVERSITY OF TECHNOLOGY

FAKULTA STROJNÍHO INŽENÝRSTVÍ
ÚSTAV MATERIÁLOVÝCH VĚD A INŽENÝRSTVÍ

FACULTY OF MECHANICAL ENGINEERING
INSTITUTE OF MATERIALS SCIENCE AND ENGINEERING

PHYSICAL AND ELECTRICAL PROPERTIES OF 0.5BA(ZR0.2TI0.8)O3-0.5(BA0.7CA0.3)TIO3 CERAMICS

FYZIKÁLNÍ A ELEKTRICKÉ VLASTNOSTI 0.5BA(ZR0.2TI0.8)O3-0.5(BA0.7CA0.3)TIO3 KERAMIK

BAKALÁŘSKÁ PRÁCE
BACHELOR'S THESIS

AUTOR PRÁCE — MICHAEL KRÁL
AUTHOR

VEDOUCÍ PRÁCE — Mgr. HANA HUGHES, Dr.
SUPERVISOR

BRNO 2015

Vysoké učení technické v Brně, Fakulta strojního inženýrství

Ústav materiálových věd a inženýrství
Akademický rok: 2014/2015

ZADÁNÍ BAKALÁŘSKÉ PRÁCE

student(ka): Michael Král

který/která studuje v **bakalářském studijním programu**

obor: **Materiálové inženýrství (3911R011)**

Ředitel ústavu Vám v souladu se zákonem č.111/1998 o vysokých školách a se Studijním a zkušebním řádem VUT v Brně určuje následující téma bakalářské práce:

Fyzikální a elektrické vlastnosti 0.5Ba(Zr0.2Ti0.8)O3-0.5(Ba0.7Ca0.3)TiO3 keramik

v anglickém jazyce:

Physical and electrical properties of 0.5Ba(Zr0.2Ti0.8)O3-0.5(Ba0.7Ca0.3)TiO3 ceramics

Stručná charakteristika problematiky úkolu:

Příprava keramických kompozic. Studium vlivu velikosti zrn 0.5Ba(Zr0.2Ti0.8)O3 - 0.5(Ba0.7Ca0.3)TiO3 keramik na fyzikální a elektrické vlastnosti.
Cíle, kterých má být dosaženo:
a) příprava keramických kompozic 0.5Ba(Zr0.2Ti0.8)O3-0.5(Ba0.7Ca0.3)TiO3 (mixed oxide route)
Kompozice 0.5Ba(Zr0.2Ti0.8)O3-0.5(Ba0.7Ca0.3)TiO3
b) měření velikosti částic připravených keramických kompozic 0.5Ba(Zr0.2Ti0.8)O3 - 0.5(Ba0.7Ca0.3)TiO3, XRD analýza
c) slinování připravených keramických kompozic
d) měření fyzikálních a elektrických vlastností

Cíle bakalářské práce:

Příprava a slinutí 0.5Ba(Zr0.2Ti0.8)O3-0.5(Ba0.7Ca0.3)TiO3 keramické kompozice s následným studiem jejich fyzikálních a elektrických vlastností.

Seznam odborné literatury:

1) S.Qiao, J.Wu, B.Wu, B.Zhang, D. Xiao, J.Zhu; Effect of Ba0.85Ca0.15Ti0.9Zr0.1O3 content on the microstructure and electrical properties of Bi0.51(Na0.82K0.18)0.50TiO3 ceramics; Ceram.,Int.(2012) article in press
2) P.Wang, Y.Li, Y.Lu; Enhanced piezoelectric properties of (Ba0.85Ca0.15)(Ti0.9Zr0.1)O3 lead free ceramics by optimizing calcination and sintering temperature; J. Eur.Cer.Soc. 31 (2011) p. 2005-2012
3) J.Wu, D.Xiao, B.Wu, W.Wu, J.Zhu, Z.Yang, J.Wang; Sintering temperature- induced electrical properties of (Ba0.9Ca0.1)(Ti0.85Zr0.15)O3 lead free ceramics; Mat. Res. Bul. 47 ((2012) p.1281-1284
4) W.Liu, X.Ren; Large piezoelectric effect in Pb-free ceramics, Phys.Rev.Lett. 103 257602 (2009)
5) Electroceramics: Materials, Properties, Applications, Second Edition

Author(s): A. J. Moulson, J. M. Herbert
Published Online: 1 SEP 2003
Print ISBN: 9780471497479
Online ISBN: 9780470867969
DOI: 10.1002/0470867965

Vedoucí bakalářské práce: Mgr. Hana Hughes, Dr.

Termín odevzdání bakalářské práce je stanoven časovým plánem akademického roku 2014/2015.

V Brně, dne 31.3.2015

L.S.

prof. Ing. Ivo Dlouhý, CSc.	doc. Ing. Jaroslav Katolický, Ph.D.
Ředitel ústavu	Děkan fakulty

ABSTRACT

The purpose of this study is to prepare lead-free piezoelectric powders and ceramics with composition $0.5Ba(Zr_{0.2}Ti_{0.8})O_3$-$0.5(Ba_{0.7}Ca_{0.3})TiO_3$ and subsequent measurement of their physical and electrical properties. This thesis contains a literature review about piezoelectric ceramics and their properties, together with a description of the experimental approach to the preparation and measurement of properties of the samples. Contributions of the thesis are an exact description of the fabrication and measurement of properties, determination physical and electrical properties of this lead-free piezoceramic and suggestions for further development. The best electrical properties were measured on samples sintered at a temperature of 1425 °C, with d_{33} = 290.5 pC/N, average value of grain size is 46.8 μm and relative density of 93.9 %.

Key words

lead-free materials, piezoceramics, Bi-doped ceramics, piezoelectric properties, piezoelectric materials

ABSTRAKT

Účelem této práce je příprava prášku a bezolovnaté keramiky se složením $0,5Ba(Zr_{0,2}Ti_{0,8})O_3$-$0,5(Ba_{0,7}Ca_{0,3})TiO_3$ a následné měření jejích fyzikálních a elektrických vlastností. Práce obsahuje literární rešerši na téma piezokeramické materiály a jejich vlastnosti, společně s experimentální částí, která popisuje přípravu a měření vlastností vzorků. Přínosy práce jsou přesný popis výroby a měření vlastností, stanovení fyzikálních a elektrických vlastností této bezolovnaté piezoelektrické keramiky a návrhy na další vývoj. Nejlepší elektrické vlastnosti byly naměřeny na vzorcích slinovaných při teplotě 1425 °C a to d_{33} = 290.5 pC/N, průměrná velikost zrn 46.8 μm a relativní hustota 93.9 %.

Klíčová slova

bezolovnaté materiály, piezokeramiky, keramiky dopované Bi, piezoelektrické vlastnosti, piezoelektrické materiály

BIBLIOGRAPHIC CITATION

KRÁL, M. *Physical and electrical properties of 0.5Ba(Zr0.2Ti0.8)O3-0.5(Ba0.7Ca0.3)TiO3 ceramics.* Brno: Brno University of Technology, Faculty of mechanical engineering, 2015. 54 p. Thesis Supervisor Mgr. Hana Hughes, Dr.

DECLARATION OF AUTHENTICITY

I, declare that I prepared this bachelor's thesis independently using literature and sources, which are shown in the list of references.

Datum	Michael Král

ACKNOWLEDGEMENT

At this point I would like to thank my thesis supervisor Mgr. Hana Hughes, Dr. for her guidance and valuable advices. Also I want to express my thanks to Ing. Aleš Matoušek, Ph.D. for his guidance in laboratory. I would like to thank everyone who helped me with the preparation and evaluation of samples. I would also like to thank my family and girlfriend for their support.

Contents

List of abbreviations

Abbreviation	Description
AC	Alternating current
BCTZ	Composition (1-*x*)$Ba(Zr_{0.2}Ti_{0.8})O_3$-*x*$(Ba_{0.7}Ca_{0.3})TiO_3$
BNKT	Composition $Bi_{0.5}(Na_xK_{1-x})_{0.5}TiO_3$
BNT	Composition $Bi_{0.5}Na_{0.5}TiO_3$
DC	Direct current
KNN	Composition (K, Na)NbO_3
MPB	Morphotropic phase boundary
PEG	Polyethylene glycol
PS	Polystyrene
PT	Composition $PbTiO_3$
PVA	Polyvinyl alcohol
PVF_2	Difluoropolyethylene
PVDF	Polyvinylidenefluoride
PZ	Composition $PbZrO_3$
PZT	Composition $Pb(Zr_xTi_{1-x})O_3$
SEM	Scanning electron microscope

List of symbols

Symbol	Description
D	Electric induction
E	Electric field strength
K^T	Dielectric constant
P	Polarization
T	Mechanical stress
T_C	Curie temperature
T_{sint}	Sintering temperature
S	Mechanical strain
d	Piezoelectric constant
g	Voltage constant
k_p	Coupling factor
m	Mass
s	Elastic compliance
ε	Absolute permittivity
ε_0	Permittivity of vacuum
ε_r	Relative permittivity
ρ	Density
tan δ	Dissipation factor
at.%	atomic percent

List of figures

List of tables

1. Introduction

Piezoelectric ceramics are key materials in many sensor and actuator applications and are used widely in practically all areas of everyday life including transport, energy, healthcare, communications and the home environment. The piezoelectric effect was first discovered in single crystal materials in the late nineteenth century. But first utilization came during the Second World War with the arrival of new polycrystalline piezoelectric ceramics. Since the 1950's Lead Zirconate Titanate (PZT) has been used. [1, 2, 3]

Lead-based piezoelectric materials have dominated the commercial market for electromechanical devices for more than half a century, because of their superior piezoelectric properties. However, the environmental pollution caused by highly toxic lead has induced an urgent need in developing lead-free piezoelectric materials for the demands of various applications. [3, 4]

In 2009 Liu and Ren published an article about a new piezoelectric composition named $(1\text{-}x)Ba(Zr_{0.2}Ti_{0.8})O_3\text{-}x(Ba_{0.7}Ca_{0.3})TiO_3$, abbreviated as BCTZ. It shows further promise in the area of lead-free piezoelectric ceramics as their properties are comparable to standard lead-based materials. [5]

2. Literature review

2.1. Piezoelectricity

2.1.1. Piezoelectric effect

The piezoelectric effect is the ability of certain materials to generate electric charge during distortion. There exists a direct and an indirect piezoelectric effect. The direct piezoelectric effect means polarization (*P*) is developed by a stress (*T*). It is represented by the following formula $P = dT$, where *d* is the piezoelectric charge constant. The indirect effect means strain (*S*) is developed by an electric field (*E*). It is represented by the following formula $S = dE$. [1, 6]

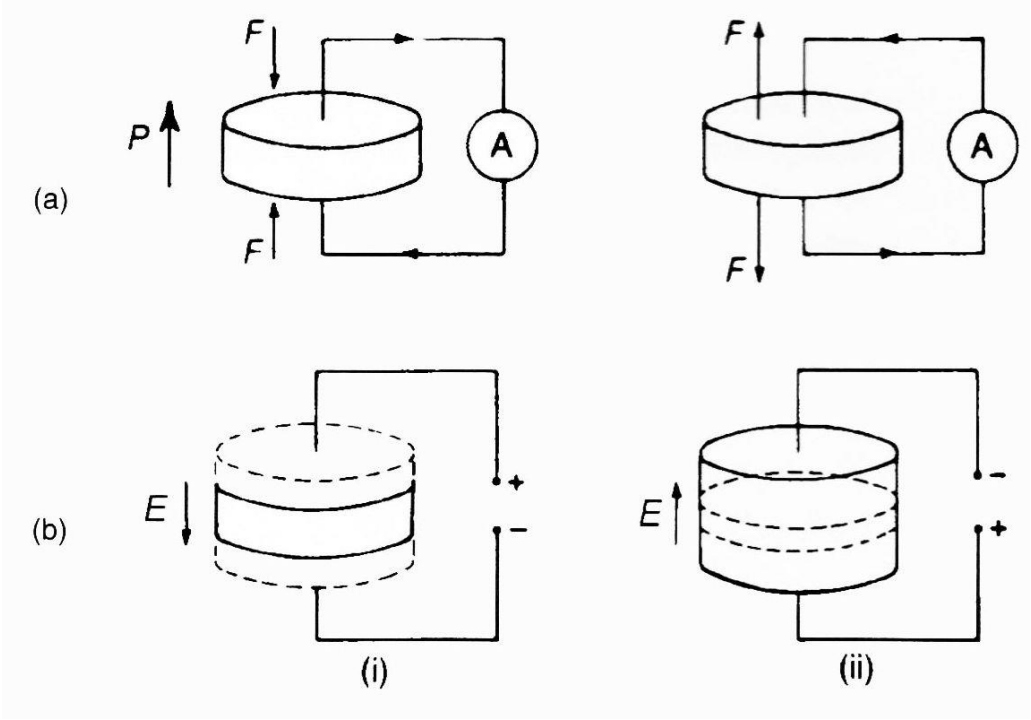

Fig. 2.1 (a) The direct and (b) inverse piezoelectric effect: (i) contraction; (ii) expansion. The broken lines indicate the original dimensions. [1]

2.1.2. Ferroelectricity

Ferroelectric materials are a group of materials which have a spontaneous electric polarization, that can by reversed by the application of an external electric field. There are areas in material where dipole moments are equally oriented. These dipole moments stay in the material even if we disconnect the external electric field. Direction of the polarization vector can be changed by an electric field. Similar type of materials is Pyroelectric materials which change their polarization by changing the temperature. Each ferroelectric material has a piezoelectric behavior, but not all of piezoelectric materials are ferroelectric materials. [11]

The ferroelectric materials exhibit ferroelectric behavior only below the phase transition temperature (Curie temperature Tc), above this temperature, these materials are paraelectric. [2, 11, 12]

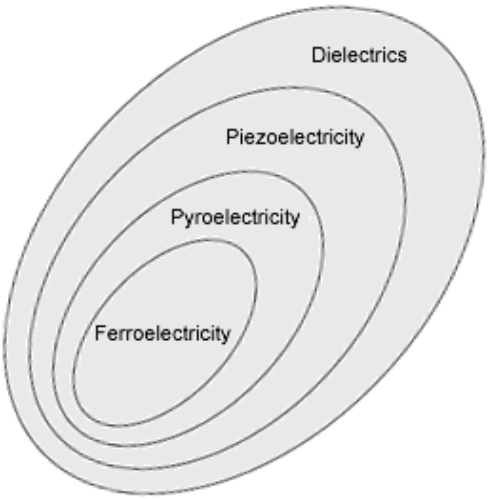

Fig. 2.2 The subgroups of dielectrics.

Ferroelectric polarization describes the hysteresis loop, which is dependent of the size of polarization (*P*) on the intensity electric field (*E*), example of hysteresis loop you can see in Figure 2.3.

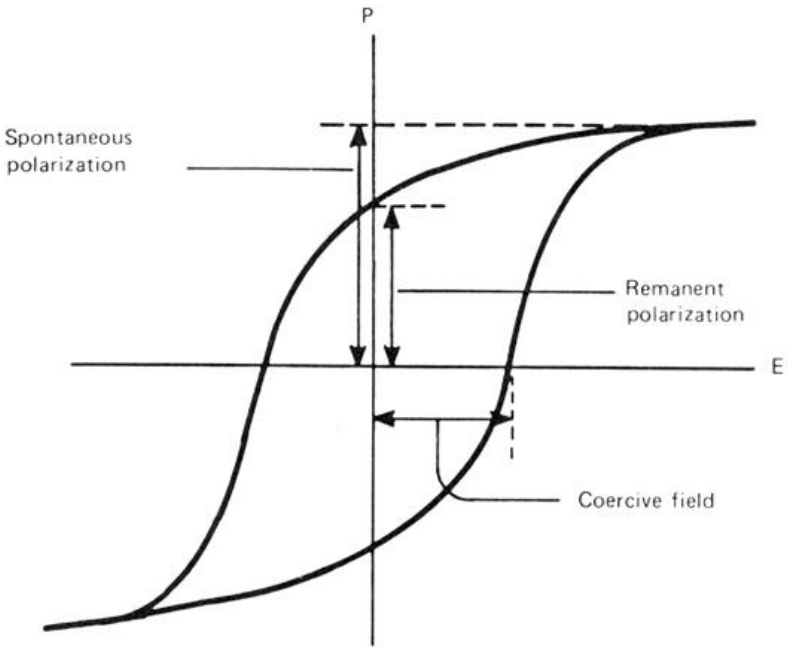

Fig. 2.3 Hysteresis loop of ferroelectric material.

2.1.3. Origin of piezoelectric effect

Piezoelectric properties are exhibited only in non-centrosymmetric crystals. Crystals are composed of ions. Ions in cells without center of symmetry can arrange themselves so that the center of the positive and negative charges are not coincident, and can be influenced during the application of mechanical stress. It causes the creation of dipoles in material. Such dipoles cannot exist in crystals with a center of symmetry. The origin of this effect is in crystal without mechanical stress the positions of positive and negative charge centers are the same. During

mechanical stress, the positions of the charge centers are changed, creating a dipole. Dipole moments exist in the crystal only during mechanical stress. Overall crystal is still electrically neutral, even with a dipole. [1, 6]

The size of created electric charge is linearly dependent on the magnitude of the mechanical deformation. [1, 2] Of course size of electric charge is dependent on quality of piezoceramic, shape and size of the testing piece and size and location action of the external strain. [1, 6]

2.1.4. History of piezoelectricity

The direct piezoelectric effect was first demonstrated by brothers Pierre and Jacques Curie in 1880. Brothers Currie had knowledge of crystallography and both were excellent physicists. Using knowledge of the Pyroelectric effect and internal structures of crystals they prepared experiments with crystals of Tourmaline (aluminum borosilicate of iron) and the results demonstrated the direct piezoelectric effect. [2, 6, 7] Indirect piezoelectric effect was mathematically predicted by Gabriel Lippmann in 1881. Later it was proved experimentally by brothers Curie. [6] Research culminated in 1910 when Woldemar Voigt wrote a publication Crystal Physics, where he described 20 natural crystals, which have piezoelectric properties. He rigorously defined their piezoelectric constants. [1, 6, 8]

The first device containing piezoelectric components was sonar. Sonar was invented in 1917 during World War I. in France by Paul Langevin. The success of sonar caused further development of piezoelectric materials. In the interwar period the piezoelectric parts began to acquire usage in other applications such as gramophones and radios. During World War II. was invented a new class of synthetic ferroelectric materials, which had significantly better piezoelectric properties than natural crystals. Between these materials were $BaTiO_3$ and $Pb(Zr_xTi_{1-x})O_3$, abbreviated as PZT. That led to research and development of synthetic piezoelectric ceramics. This ceramics quickly received wide usage in radio electronics, automation, telecommunication, IT technology, medicine, aviation, aerospace and military technology. [2, 6]

Presently the subjects of research are improving piezoelectric properties, finding new lead-free piezoceramics, increasing efficiency amd improve thermal stability. [2]

2.1.5. Variables and constants

- **Mathematical description**

Piezoelectricity is the combined effect of the electrical and mechanical behavior of the material [9, 10]:

$$D = \varepsilon * E\,, \tag{1}$$
$$S = s * T\,, \tag{2}$$

where D …… electric induction,
ε …… permittivity,
E ..... electric field strength,
S …… mechanical strain,
s ……. elastic compliance,
T ……. mechanical stress.

- **Permittivity**

Permittivity is degree of proportionality between the intensity of the electric field (E) and the electric induction (D) inside the dielectric. Designation of absolute permittivity is ε.

Absolute permittivity is product of multiplication of the permittivity of vacuum ($\varepsilon_0 = 8.854 \cdot 10^{-12}$ Fm^{-1}) and the relative permittivity of the material (ε_r). [9]

When describing piezoelectric ceramic is often used dielectric constant K^T. [1, 6, 9]

$$K^T = \frac{\varepsilon_{33}^T}{\varepsilon_0} \; [-], \tag{3}$$

where ε_{33}^T ..... permittivity is indicate under constant mechanical stress in the third axis.

- **The piezoelectric charge coefficient**

This coefficient has designation *d*. Another possible designation is d_{ij}, where *i* is the axis in which the electric charge is generated and *j* is the axis in which the mechanical stress is applied or observed. This coefficient describes size of electrical charge, which is generated in material under mechanical stress. This coefficient is the most important for piezoelectric materials. [1, 9]

$$d = \frac{strain\ development}{applied\ electricfield} = \frac{short\ circuit\ charg\ edensity}{applied\ mechanical\ stress} \; [\mathrm{pC} * \mathrm{N}^{-1}] \tag{4}$$

- **Young's modulus of elasticity**

The modulus of elasticity describes the elasticity of material. It is the ratio of mechanical stress and mechanical deformation. Designation of the modulus is *E*. [6]

$$E = \frac{\sigma}{\varepsilon} = \frac{mechanical\ stress}{relative\ deformation} \quad [\mathrm{Pa}] \tag{5}$$

2.2. Piezoelectric materials and applications

A boom of piezoelectric materials began in the twentieth century during the 1950s and 1960s. At that time research and mass production were started. Previously, it was only possible to gain piezoelectric components from natural crystals. Currently, piezoelectric components are made from polycrystalline substances called piezoceramics and are produced industrially. [6]

The research focuses on improving properties, like better temperature stability, better efficiency or lower supply voltage. Last but not least, much of the research is dedicated to finding new and better materials. [6]

2.2.1. Piezoelectric effect in crystals

Crystals were the first materials to be discovered with piezoelectric properties. Among the most popular materials belonged to the sixties of the twentieth century. The most famous of these crystals are quartz (SiO_2) and Tourmalines. Another used minerals were Lithium niobate ($LiNbO_3$), Berlinite ($AlPO_4$), Lithium tantalate ($LiTaO_3$) or Germanium bismuth ($Bi_{12}GeO_{20}$) etc. [6, 13]

- **Tourmalines**

Tourmaline is mineral occurring in nature in many modifications. Piezoelectric behavior was first demonstrated on the Tourmaline. Its symmetry is oriented only to the axis z. Tourmaline is used for example in sensors. Tourmaline has similar properties like quartz, but it is very dependent on the temperature because it has pyroelectric behavior as well. [6]

- **Quartz**

Quartz is one of the most common minerals in the earth's crust. It was the first industrially used piezoelectric material. Quartz is chemically resistant and it has good mechanical properties and it is resistant to high pressures. Quartz was originally mined from the nature. However their properties are not suitable for commercial applications. Therefore, the technically used quartz is produced artificially. Advantages of quartz are stability even at high temperatures (about 573 °C), high hardness etc. Disadvantage is worse piezoelectric properties than piezoceramics. [6]

2.2.2. Piezoelectric ceramics

Piezoceramics are artificially created materials with piezoelectric properties. They are polycrystalline materials. Artificially produced piezoceramics have an exact composition. [6]

First of piezoceramics were barium titanate (BaTiO3), lead titanate ($PbTiO_3$), lead zirconate ($PbZrO_3$) and of course the most widely used combination of these compositions PZT ($Pb(Zr_xTi_{1-x})O_3$). These materials have better properties and lower price than piezoelectric crystals for some applications. Therefore piezoceramic acquires wide use in various applications. Most of these materials have the Perovskite structure, which imparting good piezoelectric properties. [14] Advantage of piezoceramics is high value of piezoelectric constants. The biggest disadvantage of this material is relatively low Curie temperature. [6]

2.2.3. Perovskite structure

Name for this group of structures comes from the name of nature mineral Perovskite ($CaTiO_3$) which has this type of structure. This structure is adopted by many oxides. Perovskite structure has the chemical formula ABO_3. In basic cubic cell A and B most often represent

cation with oxidation number +2 and cation with oxidation number +4, respectively. O is oxygen with oxidation number -2. [2]

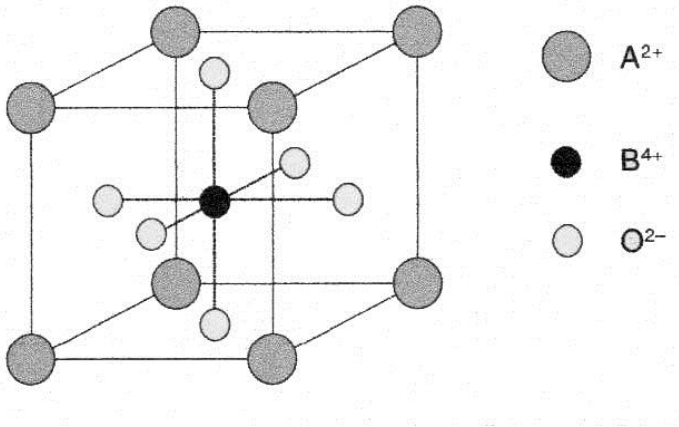

Fig. 2.4 Basic cell of perovskite structure. [2]

Materials with perovskite structure exhibit many interesting properties. For example colossal magnetoresistance, ferroelectricity, superconductivity etc. [2, 11]

2.2.4. Morphotropic phase boundary

The term MPB (Morphotropic phase boundary) was previously used for area of chemical composition of the solid solution, where in wide temperature range two phases can coexist. [2] Nowadays, MPB is used to refer to the phase transition between the tetragonal and the rhombohedral ferroelectric phases as a result of varying the composition or as a result of mechanical pressure. [11]

Just around MPB material has the best piezoelectric properties. Therefore we try in the production of piezoelectric materials to obtain chemical composition close to the MPB. [2] Common ferroelectric materials which use MPB are complex-structured solid solution. The most widely used piezoelectric material is system based on $Pb(Zr_{1-x}Ti_x)O_3$ (PZT), a solid solution of $PbZrO_3$ and $PbTiO_3$ as shown in Fig 2.5.

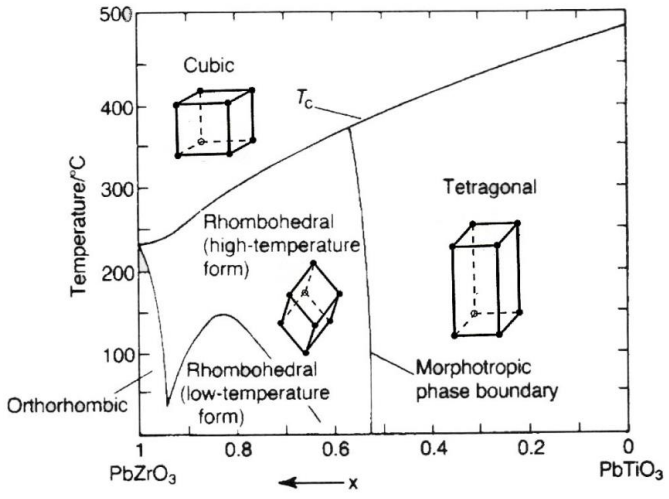

Fig. 2.5 Phase stabilities in the system $Pb(Ti_{1-x}Zr_x)O_3$. [1]

2.2.5. Curie temperature

Different piezoelectric materials have different Curie temperature (T_c). For example $PbZrO_3$ has T_c = 230 °C, $PbTiO_3$ has T_c = 490 °C and $BaTiO_3$ has T_c = 130 °C. Disadvantage of current lead-free piezoelectric ceramic is its low T_c only about 100 °C. This temperature is critical for piezoelectric behavior, because T_c is the interface between ferroelectric and paraelectric phases of material. This means the ferroelectric of piezoelectric material loses its beneficial properties. At this temperature the crystal structure changes from non-symmetrical to symmetrical and this transformation causes loss of piezoelectric and ferroelectric properties. [2, 5, 9, 11] Note that the direction of polarization is different in the different ferroelectric phases (Fig 2.6).

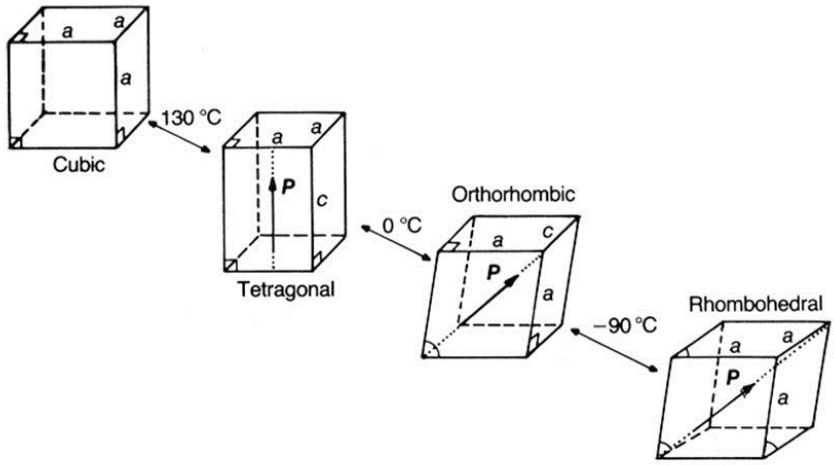

Fig. 2.6 Changes of crystal structure of$BaTiO_3$depending on the temperature. [1]

2.2.6. New developments

- **Polymers**

Piezoelectric behavior of these materials was discovered at 1969. The most widely used of these materials are polyvinylidenefluoride (PVDF) and difluoropolyethylene (PVF_2). Piezoelectricity occurs in polymers due to anisotropy. Part of the polymer is in the form of crystals and part is in the form amorphous chains. Polymers have better piezoelectric properties than quartz. Their advantages are the possibility of working with high voltage, easy production, pliability and elasticity. Organic polymers are used for sensitive sensors of vibration. [6, 13]

- **Ceramic-polymer composites**

Composite piezoelectric materials are materials, in which at least one component has piezoelectric properties, and the resulting properties are usually better than either of the materials individually. Composite foundation is usually ceramic, but it is not the rule. [6]

Connection of polymer and piezoceramic can mean resolving the disadvantages of both materials. Ceramics are fragile and hard but have better piezoelectric properties than polymers. Polymers are flexible and tough. Composite technology in general sets out to combine materials in such a way that the properties of composite are optimum for a particular application. The property, whether mechanical, thermal, electrical etc., is determined by the choice

of component and their relative amounts and, most importantly, the 'connectivity', that is the manner in which the components are interconnected. [1]

There are eight different types of two-phase piezocomposites (0-3, 1-3, 2-2, 2-3, 3-0, 3-1, 3-2 and 3-3). The firs number in the notation denotes the physical connectivity of the active phase and the second number refers to the physical connectivity of the passive phase. [18] There are two commonly used connections, 0-3 and 1-3. [1]

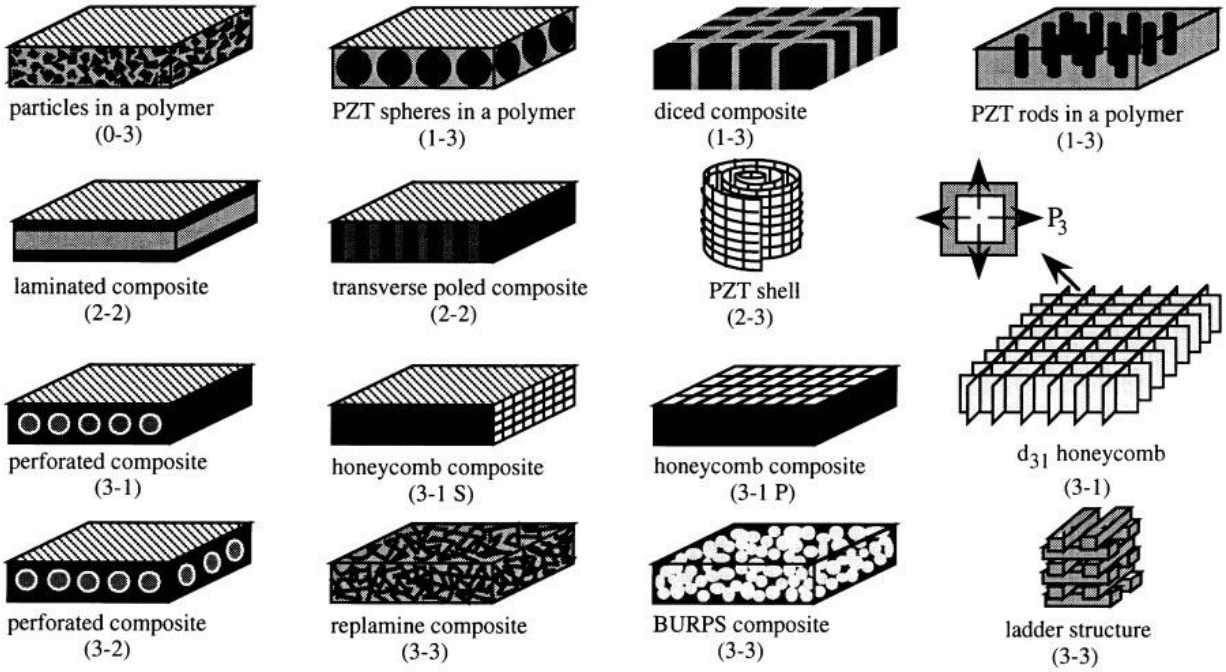

Fig. 2.7 Connectivity of constituents in piezoelectric ceramic-polymer composites. [18]

- *Composites with 1-3 connectivity*

  The composites with 1–3 connectivity are the most studied and utilized of all the two-phase connectivity types. This composite consists of individual PZT rods or fibers aligned in a direction parallel to the poling direction and surrounded by a polymer matrix. The rod diameter, rod spacing, composite thickness, volume percent of rods, and polymer compliance all influence the composite performance. [18]

- *Composites with 0-3 connectivity*

  Composites with 0–3 connectivity consist of a random array of piezoelectric particles dispersed in a 3D polymer matrix. The primary advantage of these composites is their ability to be formed into shapes while remaining piezoelectrically active. [18]

2.2.7. Types of piezoelectric components

In applications piezoelectric materials can be formed of one or multilayer structures. [6]

- **Unimorphs**

Unimorphs are made of metal plate bonded to a piezoelectric layer and contacts. Unimorphs are used in electroacoustic transducers and sensors of non-electrical quantities. [13]

- **Bimorphs**

Bimorphs are made of two piezoelectric layers. It can be combined with other materials such as metal plates or plastics. There are two possible connections, series connection and parallel connection. Bimorphs are used in actuators and sensors. [9, 13]

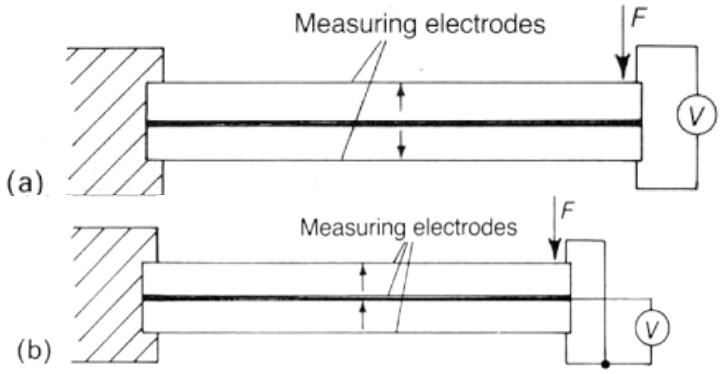

Fig. 2.8 Cantilever bimorphs showing (a) series connection and (b) parallel connection of beams. [1]

- **Multi-layer materials**

Multilayered piezoelectric components with high energy conversion efficiency. Multi-layer materials are used in actuators in low-energy applications and applications with large displacements whist requiring low actuating voltages. [13]

2.2.8. Applications of piezoceramics

Piezoceramics have wide usage.in a range of applications as shown in Figure 2.9. Some applications for example ultrasound transducers utilize both the direct and the indirect piezoelectric effects. Important applications will be further discussed in more details.

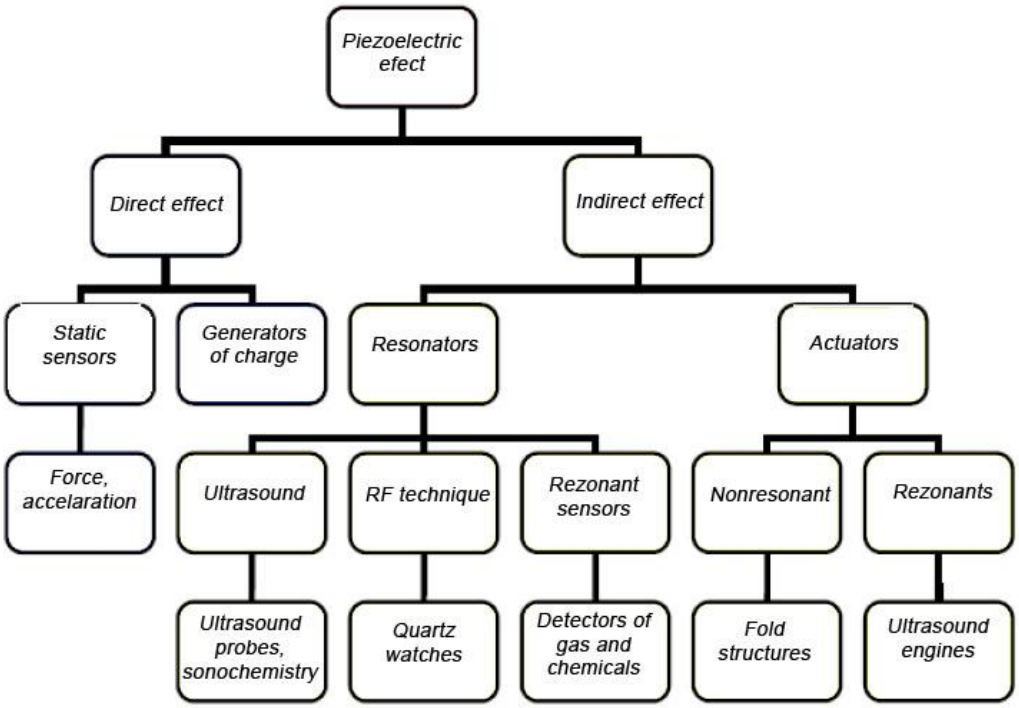

Fig. 2.9 Division of uses the piezoelectric effect. [6]

❖ **Generators**

These systems use mechanical energy from the surroundings, such as vibration, acoustic noise, movement of the human body and can generates electric charge, which can then be used to generate a voltage. [6]

Piezoelectric generators are several types. Pressure piezoelectric generators operate on the principle of compression. During compression a small voltage is generated. This type of generator is used for example in the gas lighter or in heels of shoes. During the walk you can generate power. Vibration generators use vibration of the surroundings. There are three types of vibration piezogenerators. First type uses vibration from seismic inertia. Resulting electric charge is generated by compressing and stretching of piezoelectric component. Electric charge is directly proportional to stress. The second type uses torsional oscillations of piezoelectric rollers. The third type uses fixed beam, which free end oscillates and piezoelectric component is stretched and compressed, for example using the cantilever structures described above [6]

❖ **Sensors**

Sensors convert vibrations, upheavals, pressure or acoustic waves to the electric signal. They are usually small and very sensitive components. The ability to capture even the most subtle vibrations is more important than the production of power. It is difference between generators and sensors. Like piezoelectric materials in sensors are used for example quartz in certain crystallographic orientations, piezoelectric composite or polycrystalline ceramics. [6]

Piezoelectric sensors are used in safety sensors, sensors of sound in acoustic guitars, pressure gauges etc. [6]

❖ **Motors and actuators**

Piezoelectric actuators are used in applications with AC power with excitation which has own value of frequency. Microactuator produces movement which creates piezoelectric motor. Linear or rotary movement of the engine is achieved by friction forces. Friction forces are a result of generated displacements. These motor can be used only for small movements. Advantages of piezoelectric motors are high density of power, precise control, quiet operation, absence of magnetic field and construction simplicity. These components are used for example in printers and microengines. [6]

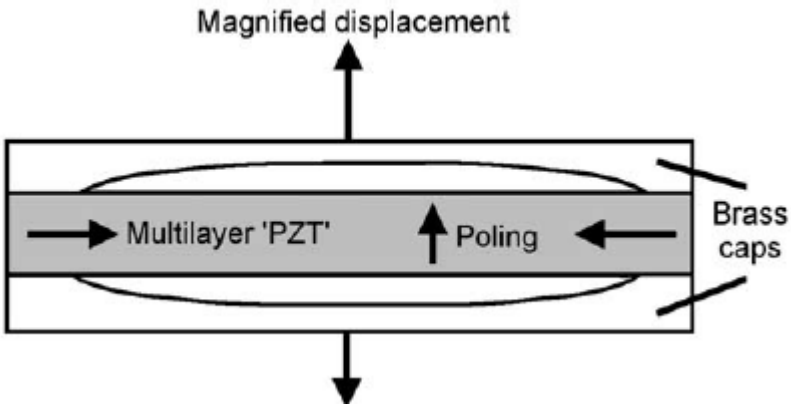

Fig. 2.10 The 'Moonie' actuator. [1]

❖ **Sonic and Ultrasonic devices**

Sonic or ultrasonic waves are energized and received by piezoelectric transducer. Incoming wave is changed to electric signal in the transducer and conversely acoustic energy can be produced by the application of a suitable electrical impulse. Properties and quality of the generated waves are given by shape and the ratio of characteristic dimensions of the piezoelectric body to wavelength. Important parameter of transducer is his resonant frequency. These devices are used in microphones, speakers, buzzers, sonars etc. [6]

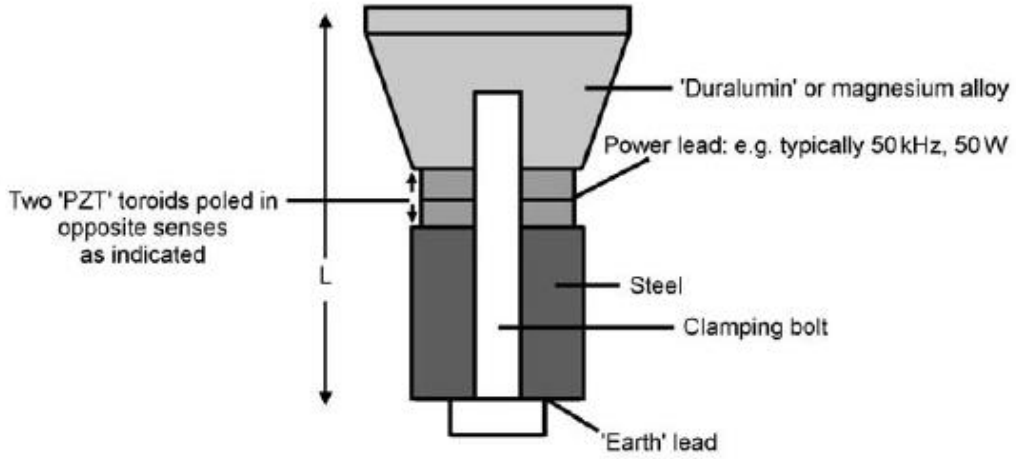

Fig. 2.11 The essentials of a power transducer for ultrasonic cleaning (the component is cylindrically symmetrical about the vertical axis). [1]

2.3. Fabrication of piezoelectric ceramics

The objectives of fabrication are to produce: [1]

1. a material with specific properties
2. a body of a required shape and size specified dimensional tolerances
3. the required component at an economic cost

Properties of ceramic are affected by composition, purity, grain size, porosity and density of the sintered ceramic. Fabrication of piezoceramics has big impact on the resulting properties too. The most important steps during fabrication are calcination and sintering. During these processes the free energy of the system goes down. New phases are formed, the particle surface area decreases and grain size increases. Always the sample shrinks. It is important that the sample shrinks throughout the volume as well otherwise the shape will be distorted. [1]

The fabrication process comprises five stages: [1]

1. The specification, purchase and storage of raw materials
2. The preparation of a composition in powder form
3. Forming the powder into a shape
4. Densification
5. Finishing

2.3.1. Solid state route

Process begins with precision weighing of raw materials followed by mixing and grinding of these materials. Raw materials must be high purity about 95.5 %. The impurities cause degradation of the properties. Starting materials are oxides for example PbO, ZrO_2 and TiO_2 to produce PZT powder or $BaCO_3$, BaO and TiO_2 to produce $BaTiO_3$ powder. Quantity of oxides is calculated by stoichiometric ratio dependent on the desired composition. The weighed powders are ball - milled on a horizontal mill in an aqueous or non-aqueous solution with milling media, where mixing and milling of the powders is achieved. The particles of powder are mixed up and big agglomerates are broken down. The next step is calcination at elevated temperature. During calcination, a chemical reaction takes place to form the appropriate solid solution with the required composition and phase structure. After calcination the calcined powders are milled again in aqueous or non-aqueous solution with milling media. After each milling the mixture must be thoroughly dried. The milling media must be cleaned thoroughly after each milling and dried to prevent any possible contamination. The particle size is measured during the milling process to be able to control and achieve the required particle size for further product development. The sizes of the particles vary from 1 to 10 μm. The last step is the addition of organic binders (for example PEG, PVA) which will allow much better shaping or forming of the powders to the desired shape. Shape of green body is created by pressing into molds, extruding or tape-casting, depending on the shape required. In Figure 2.12 can be seen a schematic diagram of uniaxial dry pressing. Other methods can be seen in Table 2.1. [1, 2, 17]

Tab. 2.1 Feed materials for various shaping methods and the type of product. [1]

Shaping method	Type of feed material	Type of shape
Dry-pressing	Free-flowing granules	Small simple shapes
Isostatic pressing	Fragile granules	Large more intricate shapes
Calendering; viscous plastic proccesing	Plastic mass based on an elastic polymer	Thin plates; Simple shapes
Extrion	Plastic mass using a viscous polymer solution	Elongated shapes of constant cross-section
Jiggering	Stiff mud containg clay	Large simple shape
Injction moulding	Organic binder giving fluidity when hot	Complex shapes
Slip-castig	Free-flowing cream	Mainly hollow shapes
Band-casting	Free-flowing cream	Thin plates and sheets
Screen-printing	Printing ink consistency	Thin layers on substrates

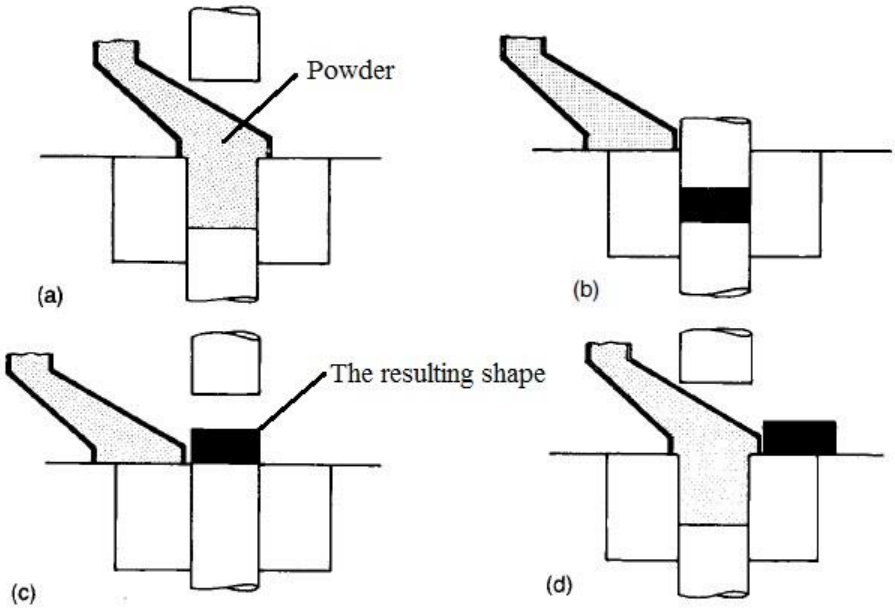

Fig. 2.12 The stages in dry pressing. [1]

After shaping the ceramics are ready to be sintered. The sintering is a process for forming a dense mass by heating compacted powders. [12] The binder burns out at high temperature around 500 °C, depending on the type of binder. The density grows and size of pores decreases during sintering of samples. Finished samples can be conventionally machined to the desired shape. The last step of fabrication is deposition of electrodes (sputtering of Au or Pt electrodes or method called screen-plating) and poling. Solid state route is commercially the most widely used method of preparing electroceramic components. [1, 2, 17]

2.3.2. Calcination

Calcination causes the constituents to interact by interdiffusion of their ions and so reduces the extent of the diffusion that must occur during sintering in order to obtain a chemically homogeneous body. The calcination conditions are important factors controlling the fabrication process. The required final phases may not be completely formed but the remaining chemical gradients may assist sintering. The main requirement is that calcination should yield a very consistent product. Calcination can be carried out by placing the mixed powders in crucibles in a furnace. The surface of crucible is in immediate contact with the powder and is made of inert material such as Al_2O_3 or ZrO_2. The calcined material has usually undergone a limited amount of sintering and must be milled to reduce the particle size in order to give a powder or slip suitable for the shaping stage. [1]

2.3.3. Sintering

Sintering is the high-temperature treatment that causes particles to join, gradually reducing the volume of pore space between them. With finer particles, many atoms or ions are at the surface for which the atomic or ionic bonds are not satisfied. As a result, a collection of fine particles of a certain mass has higher energy than that for a solid cohesive material of the same mass. Therefore, the driving force for solid state sintering of ceramics is the reduction in the total surface area and surface energy of the powder particles. When a powdered material is compacted into a shape, the powder particles are in contact with one another at numerous sites, with a significant amount of pore space between them. In order to reduce the total energy of the material, atoms diffuse to the points of contact, bonding the particles together and eventually causing the pores to shrink. Lattice diffusion from the bulk of the particles into the neck region causes densification. Surface diffusion, and lattice diffusion from curved surfaces into the neck area between particles do not lead to densification, but can contribute to the overall sintering process. [12]

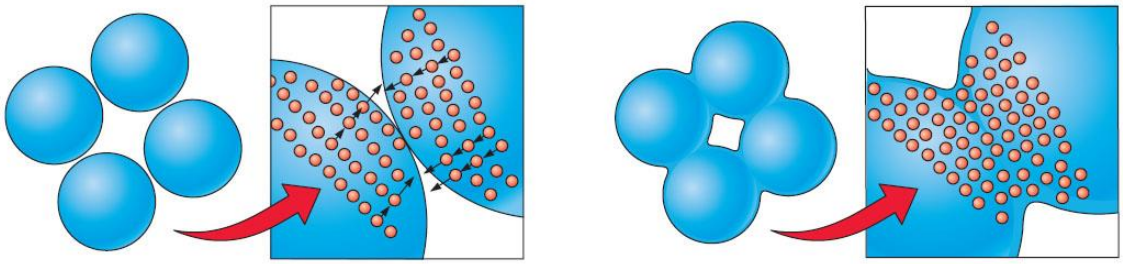

Fig. 2.13 Diffusion processes during sintering. Atoms diffuse to points of contact, creating bridges and reducing the pore size. [12]

2.3.4. Poling of piezoceramics

PZT ceramics are polycrystalline materials with various grain sizes. Ferroelectric materials like PZT contain domains in grains. Domains are areas of material where polar axis has different orientations within the allowed range of directions in the crystal system during the transformation from the paraelectric to ferroelectric phase. Ceramics with-unpoled domain structure do not show an overall piezoelectric effect. In a raw ceramic the spontaneous in the grains has different directions. This is caused by the random orientation of the grains. The domain structure can be changed by mechanical stress and electric field. In practice, the electric field (about 2 to 4 kilovolts per millimeter) is applied to the ceramics material and polarization occurs, with the polarization directions of the individual grains aligning as close as possible to the applied electric field. The best overall polarizability is attained in a material with chemical composition near the MPB, resulting in the best piezoelectric properties. It is necessary to add that all types of piezoceramic have to be poled to obtain their required piezoelectric properties. [1, 2, 7]

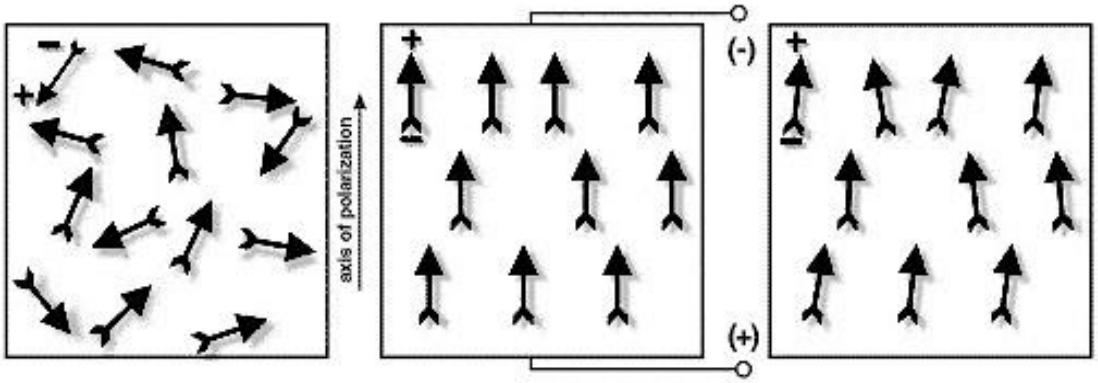

a) Random orientation of polar domains

b) Polarization in DC electric field

c) Remanent polarization after electric field removed

Fig. 2.14 Polarization (poling) a piezoelectric ceramic. [7]

2.4. Lead – based piezoceramics

Lead based piezoelectric materials are the most widely used, due to the favorable price and excellent properties. The problem with this material is that it is very difficult to recycle. Therefore toxic lead escapes to nature and causes pollution. The European Union has tried to prevent the use of lead based materials, therefore the development of new lead free piezoceramics is required. [1, 2, 4, 9]

2.4.1. PZT ceramics

Composition PZT is composed solid solutions of $PbZrO_3$ (PZ) and $PbTiO_3$ (PT). PZT has Curie temperature between 230 and 490 °C depending on the ratio of content of PZ and PT. [1, 2]

PZT composition was invented in the 1950's and development continued during the 1960s. At that time, very good material properties were discovered and PZT ceramics are among the most industrially produced piezoelectric materials. Pure PZ has trigonal symmetry and pure PT has tetragonal symmetry. PZT has perovskite structure. PZT has a composition given by the following formula $Pb(Zr_xTi_{1-x})O_3$, where most often x = 0.48 - 0.52. The Morphotropic

phase boundary (MPB) exists in the range $0.455 \leq x \leq 0.48$ at room temperature. At graph in Figure 2.15 we can see, that around MPB PZT has high value of ε_r and k_p. [1, 2, 4, 5]

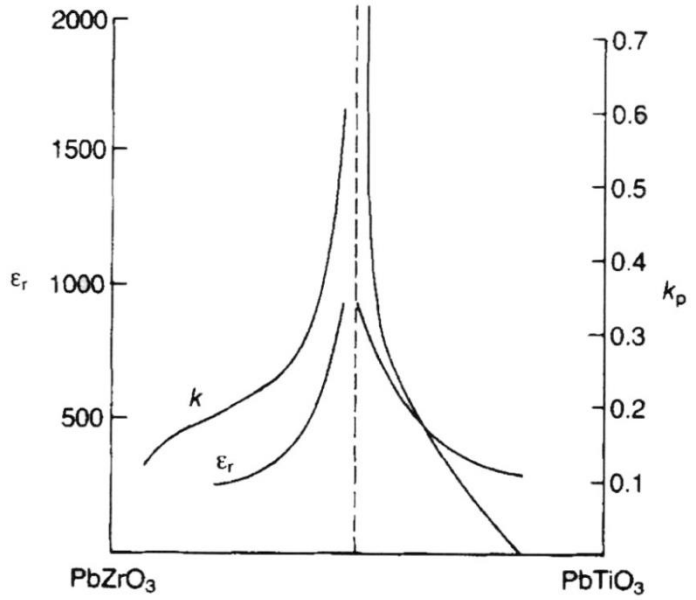

Fig. 2.15 Coupling coefficient k_p and permittivity ε_r values across the PZT compositional range. [1]

The PZT composition can be doped with a small amounts of other elements in order to improve some properties. Typical concentration of dopants are 0.05-5 at.%. It must result in the formation of dipolar pairs between an appreciable fraction of the dopant ions and the vacancies. PZT ceramics can be doped with ions to form "hard" and "soft" PZTs. It is necessary to take into account that some elements will strengthen the desired property but worsen another. Most used dopants are La, Nb and, Sr. [1, 15]

Advantages of PZT are good stability and high piezoelectric constants. Disadvantages are difficult processing, anisotropy of electromechanic properties and of course lead content. [6]

- **Soft PZT**

Soft PZT is created by donor elements, which are added to composition. Donor is element, which has one electron more than the ion it replaces. For example in place of bivalent ion A^{2+} is added trivalent ion, like La^{3+}, Bi^{3+} or Nd^{3+}. In place of quadravalent ion B^{4+} is added pentavalent ion, like Nb^{5+} or Sb^{5+}. This leads to the creation of site A site vacancies in the lattice. [6, 15] Donor – cation vacancy combinations can be assumed to have a stable orientation so that their initially random state is unaffected by spontaneous polarization or applied fields. [1]

Advantages of this type of ceramic are higher charge constant, higher permittivity and the ability to achieve greater mechanical deformation than hard piezoelectric ceramics. Soft piezoceramics are used for sensors of vibration and in acoustics. Disadvantage is low resistance to depolarization, and high losses due to domain wall movement. Due this problem it is not suitable for high electric voltage applications. [6, 15]

- **Hard PZT**

Hard PZT arises when acceptor ions are added to the composition. An acceptor ion has one electron less than the ion it replaces. For example in place of bivalent ion A^{2+} is added monovalent ion, like Ag^{+} or K^{+}. In place of quadrivalent ion B^{4+} is added trivalent ion, like Fe^{3+}, Ni^{3+} or Mn^{3+}. This is compensated for by the creation of oxygen vacancies in the lattice. [6, 15] Acceptor – oxygen vacancy combinations are likely to be less stable and thermally activated reorientation may take place in the presence of local or applied fields. The dipoles, once oriented in a common direction, will provide a field stabilizing the domain structure. [1]

Advantages of this type of ceramic are high stability, high resistance to depolarization, high value of voltage constant g_{ij}, high mechanical quality factor and low dissipation factor $tan\delta$. Due to its properties, this material is suitable for high performance applications and applications working with high mechanical stress and high electric voltage. [6, 15]

2.4.2. Fabrication of PZT

The most used method of fabrication of PZT ceramics is via the solid state route. During addition of oxide powders we want as accurate as possible composition based on stoichiometric coefficient of required composition. The best properties have ceramics with exactly required composition, without impurities and with high density. Therefore, there is a need careful control at all process stages. [1]

Basic oxide of this composition is PbO, which is volatile at temperature above 800 °C but sintering temperature is between 1200 °C and 1300 °C. Therefore calcination and sintering is usually carried out in covered crucibles with PbO-rich atmosphere (components surrounded by PbO-rich powders e.g. $PbZrO_3$). Content of PbO have to be compensated by an addition to the starting material. Other important powders are TiO_2 and ZrO_2. The TiO_2 powder reacts rapidly with PbO, and the resulting titanates only take up Zr^{4+} ions slowly from unreacted ZrO_2. These reactions occur in the solid state at temperature above 800 °C. The result is solid solution PZT. [1]

Next step is shaping and sintering. The sintered component should have a density higher than 95 % of theoretical density and a grain size in range from 5 to 30 μm. Silver electrodes are painted to the desired location and fired on at 600 - 800 °C. Ni-Cr or gold electrodes are sputtered or evaporated. Last step of fabrications is poling. [1, 2]

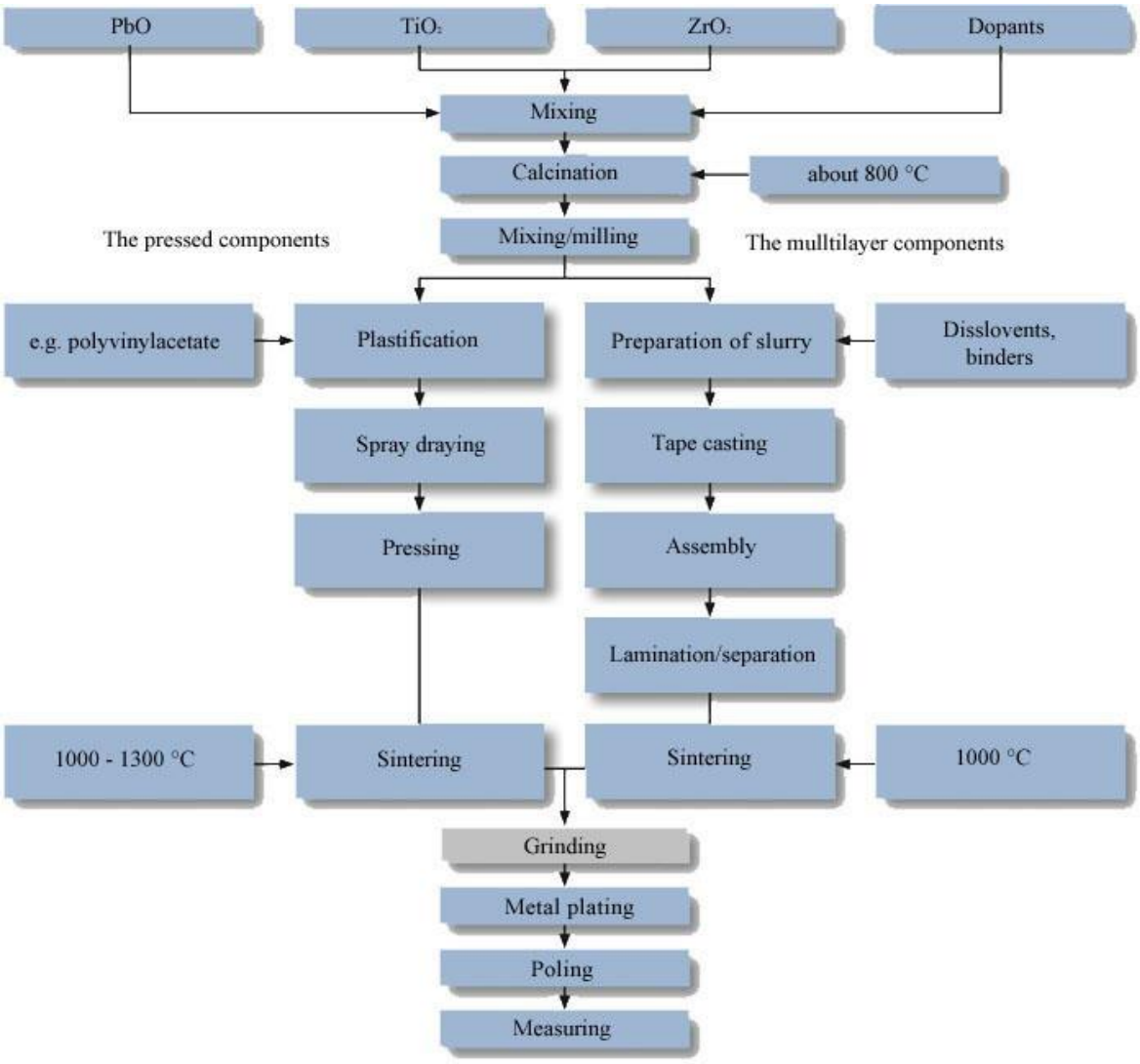

Fig. 2.16 Diagram of the fabrication process. [16]

2.5. Lead – free alternatives

The use of lead-based materials will be prohibited by the environmental regulations of the waste electrical and electronic equipment directive and the restriction of hazardous substances in Europe. [3] These regulations escalated a big boom in research of new lead free piezoelectric materials. There are previously known piezoelectric materials for example Quartz and $BaTiO_3$. And there are new piezoelectric ceramics for example $(1\text{-}x)Ba(Zr_{0.2}Ti_{0.8})O_3\text{-}x(Ba_{0.7}Ca_{0.3})TiO_3$ (BCTZ), $Bi_{0.5}(Na_xK_{1\text{-}x})_{0.5}TiO_3$ (BNKT), $(K, Na)NbO_3$ (KNN) or piezoelectric polymers in the development, but so far no lead free equivalent of PZT was found.

2.5.1. The comparison of selected piezoceramics

Tab. 2.2 Typical values of the properties of some piezoelectric materials. [1]

Property	Unit	α-Quartz[a]	$BaTiO_3$	PZT A[b]	PZT B[b]	$PbNb_2O_6$	$Na_{1/2}K_{1/2}NbO_3$	$LiNbO_3$[a]	$LiTaO_3$[a]	$PbTiO_3$[c]	PVDF
Density	$Mg\ m^{-3}$	2.65	5.7	7.9	7.7	5.9	4.5	4.64	7.46	7.12	
T_c	°C		130	315	220	560	420[d]	1210	665	494	80 (film)
ε^X_{r33}		4.6	1900	1200	2800	225	400	29	43	203	10
ε^X_{r11}			1600	1130	-	-	600	85	53	-	
tanδ	10^{-3}		7	3	16	10	10	-	-	22	0,01 (film)
k_p			0.38	0.56	0.66	0.07	0.45	0.035	0.1	-	
k_{31}			0.21	0.33	0.39	0.045	0.27	0.2	0.07	0.052	
k_{33}			0.49	0.68	0.72	0.38	0.53	0.17	0.14	0.35	
k_{15}			0.44	0.66	0.65	-	-	0.61	-	0.36	
		(11)[e] 0.1									
k_{jk}		(11)[e] 0.05									
d_{31}			-79	-119	-234	-11	-50	-0.85	-3	-7.4	
d_{33}	$pC\ N^{-1}$		190	268	480	80	160	6	5.7	47	
d_{15}			270	335	-	-	-50	69	26	-	
d_{jk}		(11)[e] 2.3									
		(11)[e] 0.67									
d_h											14
Q_m		$>10^6$	500	1000	50	11	240	-	-	326	
s^E_{11}		12.8	8.6	12.2	14.5	29	9.6	5.8	4.9	11	
s^E_{12}	$\mu m^2\ N^{-1}$	-1.8	-2.6	-4.1	-5.0	-	-	-1.2	-0.52	-	
s^E_{13}		-1.2	-2.9	-5.8	-6.7	-5 to -8	-	-1.42	-1.28	-	
s^E_{33}		9.6	9.1	14.6	17.8	25	10	5.0	4.3	11	
s^E_{44}		20.0	23	32	-	-	-	17.1	10.5	-	

[a] Single crystals.

[b] PZT A and PZT B are two typical PZT materials illustrating, in particular, the range of achievable Q_m values.

[c] + 5 mol.% $Bi_{2/3}Zn_{1/3}Mb_{2/3}O_3$.

[d] Depoles above 180 °C.

[e] Numbers in parentheses are *jk* values.

PZT A is Hard PZT and PZT B is Soft PZT

2.5.2. $BaTiO_3$

$BaTiO_3$ was the first developed piezoelectric ceramic material. Due to its properties it was used in area of the generation and detection of acoustic and ultrasonic energy. In most commercial sectors it was replaced by PZT which had superior performance. Structural transitions of this type of piezoceramic are accompanied by changes in electrical and mechanical properties. Technically pure $BaTiO_3$ has a high loss at high field strengths which is required to generate useful ultrasonic powers. $BaTiO_3$ doped with Co is used for producing high acoustic powers despite its inferior piezoelectric activity. Properties and the transition temperature can be affected by substitutions on the A and B sites. The substitution of Pb and Ca for Ba decreases the transition temperature and affects the piezoelectric properties around 0 °C which is important for underwater detection and echo sounding. The substitution Zr or Sn for Ti increase working temperature. [1]

2.5.3. $Bi_{0.5}Na_{0.5}TiO_3$

The composition $Bi_{0.5}Na_{0.5}TiO_3$ has an abbreviation BNT and it is piezoelectric ceramic. BNT is one of the candidates to replace PZT ceramics in the future. It has a perovskite structure with rhombohedral symmetry at room temperature. BNT shows strong ferroelectric properties with a relatively high Curie temperature at about 320 °C and large remnant polarization of about 38 μC/cm. Compared with PZT, BNT possesses high anisotropic electromechanical coupling properties. It used in ultrasonic applications due to its characteristics. BNT is more interesting piezoelectric material than $BaTiO_3$ because $BaTiO_3$ has relatively high sintering temperature. BNT is mostly prepared by solid state reaction routes with conventional sintering for easy synthesis and low cost. For this type of piezoceramic sintering at high temperatures unsuitable as both the Na and Bi are quite volatile. The low sintering temperature is required to maintain the stoichiometry or nominal composition with a corresponding reduction of energy consumption. [19]

2.5.4. $(K, Na)NbO_3$

The composition $(K, Na)NbO_3$ has an abbreviation KNN and perovskite structure like most of piezoelectric materials. Most often there are potassium and sodium in the ratio approximate to 1:1. KNN ceramic passes through three phase transformations. At room temperature it has an orthorhombic phase at low temperature (under 123 °C) it has a rhombohedral phase, between 200 °C and 410 °C it has tetragonal phase and above 410 °C (the Curie temperature) it has a cubic phase. There is a problem of KNN ceramic different phases has different properties and it is another possibility for research. Of course the position of the phase transformations can be changed by other elements. Pure KNN ceramics have a low d_{33} coefficient of about 80 pC/N. Good properties and value of d_{33} between 200 and 300 pC/N, KNN can be obtained after doping with other elements like Li, Ta and Sb. It also has relatively high Curie temperature. KNN ceramics can be used in the future in high-frequency ultrasonic transducers and surface acoustic wave devices. [20]

2.5.5. $Bi_{0.5}(Na_xK_{1-x})_{0.5}TiO_3$

The composition $Bi_{0.5}(Na_xK_{1-x})_{0.5}TiO_3$ is represented by abbreviation BNKT. It is lead free piezoelectric ceramic. Among the lead-free piezoelectric ceramics that have been developed, $Bi_{0.5}Na_{0.5}TiO_3$ (BNT) and $Bi_{0.5}K_{0.5}TiO_3$ (BKT) systems have received a great deal of attention due to their excellent ferroelectric and piezoelectric properties, as well being close to rhombohedral-tetragonal (MPB) compositions. In the BNT–BKT binary system, the tetragonal $Bi_{0.5}(Na_{0.78}K_{0.22})_{0.5}TiO_3$ side of the MPB composition possesses high electric field-induced strain and excellent electromechanical properties, and therefore can be considered for actuator applications. [21]

According to the literature BNKT was sintered at temperatures from 1075 °C to 1175 °C. The density was increased to temperature about 1150 °C. At 1175 °C the density declined sharply as can be seen in figure 2.17. The lower density of the BNKT ceramics sintered at 1075 °C is due to poor atomic diffusion and insufficient sintering of the ceramics. It has been demonstrated both theoretically and experimentally that the number of vacancies increases with increasing in sintering temperature. As a result, better atomic diffusion during the sintering process occurs and thus, promotes densification. However, the low density at a higher sintering temperature of 1175 °C may be due to evaporation of the volatile alkali metal. [21]

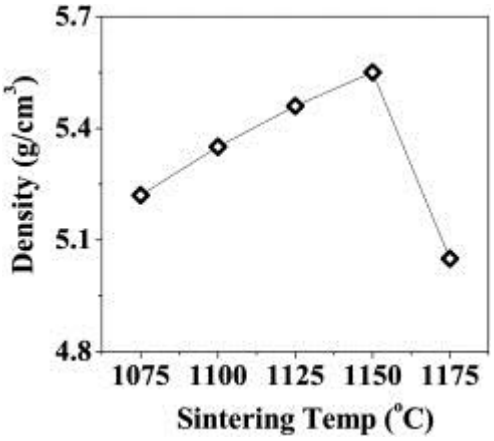

Fig. 2.17 The bulk densities of BNKT ceramics as a function of sintering temperature. [21]

BNKT ceramics sintered at an optimal temperature of 1150 °C showed high remnant polarization (P_r = 18.5 μC/cm^2) and dynamic piezoelectric coefficient (d_{33}^* = 247 pm/V). These results can be attributed to the high density and larger grain size of BNKT ceramics sintered at 1150 °C, both factors affecting the piezoelectric properties. [21]

BNKT is used as a dopant or it is doped with other elements or compositions. The literature described doping of BNKT by BCTZ. It is represented by this chemical formula $(1\text{-}x)Bi_{0.51}(Na_{0.82}K_{0.18})_{0.5}TiO_3\text{-}x(Ba_{0.85}Ca_{0.15})(Ti_{0.90}Zr_{0.10})O_3$. Temperatures of phase transitions were strongly independent on the BCTZ content. The sintering temperature and the poling electric field strongly affect the piezoelectric properties. An optimum electrical behavior of d_{33}~ 205 and k_p ~ 0.25 was demonstrated in the ceramic with x = 0.02 when sintered at 1180 °C and poled at an optimum electric field. [3]

2.5.6. $(1\text{-}x)Ba(Zr_{0.2}Ti_{0.8})O_3\text{-}x(Ba_{0.7}Ca_{0.3})TiO_3$

The abbreviation is BCTZ. Its composition and properties follows the ceramic discovered by Liu and Ren. They presented lead-free pseudobinary ferroelectric system $(1\text{-}x)Ba(Zr_{0.2}Ti_{0.8})O_3\text{-}x(Ba_{0.7}Ca_{0.3})TiO_3$, or abbreviated (1-$x$)BZT-$x$BCT where x is the molar percent of BCT. They used a conventional solid state reaction method, calcination temperature 1350 °C and sintering temperature from 1450 °C to 1500 °C in air. By measuring they discovered the existence of C-R-T triple point situated at x ~ 32 % and T ~ 57 °C as can be seen in figure 2.18. Around the triple point they measured very good piezoelectric properties. They measured high spontaneous polarization, high permittivity and high d_{33}. The relative permittivity was comparable with soft PZT materials (ε ~ 3060). Value of d_{33} was measured between 560 and 620 pC/N depending on poling conditions. This high d_{33} value even exceeds that of many soft PZTs. [5]

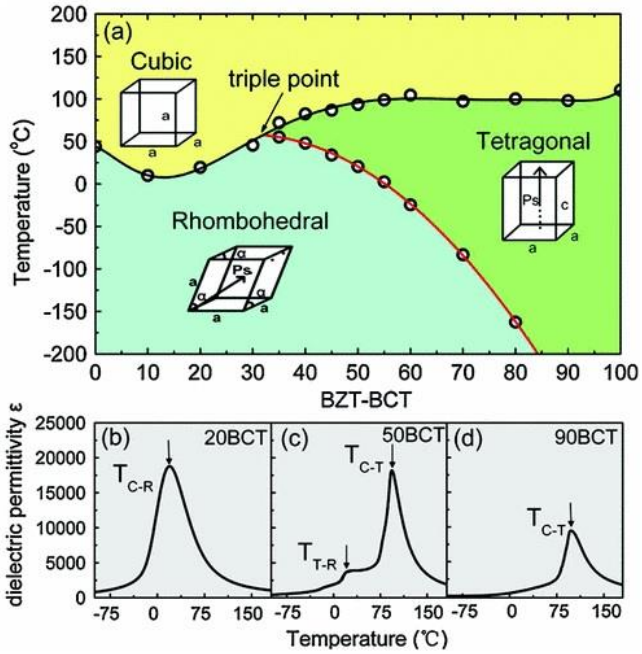

Fig. 2.18 (a) Phase diagram of pseudobinary ferroelectric system $Ba(Zr_{0.2}Ti_{0.8})O_3$-$(Ba_{0.7}Ca_{0.3})TiO_3$,abbreviated as BZT BCT. (b) - (d) Dielectric permittivity curves for 20BCT, 50BCT and 90BCT, respectively. [5]

Different authors are interested in the study of this material. They published many scientific articles on the topic. They dealt with properties of BCTZ with exact chemical composition and dependence of properties on sintering and calcination temperatures and searching for ideal values of these temperatures. They used $BaCO_3$, $CaCO_3$, ZrO_2 and TiO_2 as raw materials and they worked with this formula $(Ba_xCa_{1-x})(Ti_yZr_{1-y})O_3$. From the research results that different compositions have different properties and the best piezoelectric properties are measured at different sintering temperatures. Almost seems to be that better piezoelectric properties were measured when *x* was higher than 0,9 so ideal sintering temperature was about 1450 °C and when *x* was lower than 0,9 so ideal sintering temperature was about 1540 °C. Publications also show dependence of electrical properties, microstructure, grain size and density on calcination and sintering temperatures. In some cases, the results of BCTZ show better values than the PZT. This is the reason why BCTZ is an interesting perspective for the future. [4, 22, 23]

3. Project aims

The previous summary shows how important is research of lead-free piezoceramics and I would like to contribute to the research with my experimental part, where I deal with preparation of $0.5Ba(Zr_{0.2}Ti_{0.8})O_3$-$0.5(Ba_{0.7}Ca_{0.3})TiO_3$ piezoceramic composition and study of physical and electrical properties.

4. Experimental Approach

Preparation of the BCTZ powder was performed by conventional solid state route. Powder was milled and calcined. On prepared powder was performed phase analysis by X-ray diffraction (XRD). From prepared powder was pressed samples. Samples were sintered at temperatures from 1300 °C to 1525 °C. Sintered samples were produced on which grain size, density and some of piezoelectric properties were measured.

4.1. Used powders

As the starting raw materials were used oxides with high purity shown in Tab. 4.1. Resulting powder with composition $0.5Ba(Zr_{0.2}Ti_{0.8})O_3\text{-}0.5(Ba_{0.7}Ca_{0.3})TiO_3$ (BCTZ) was made by mixed oxide route.

Tab. 4.1 The list of powders.

Powders	Purity	Producer
$BaCO_3$	99.5%	Dakram Materials Ltd (Great Britain)
ZrO_2	99.5%	Dakram Materials Ltd (Great Britain)
TiO_2	99.5%	Dakram Materials Ltd (Great Britain)
$CaCO_3$	99.4%	Lach-ner, s.r.o. (Czech Republic)

4.2. Fabrication procedure

Fabrication procedure is composed of several steps. In the next section, the individual steps of production will be explained.

4.2.1. Weighing of powders

The raw powders were dried at 120 °C for one hour to get rid of any moisture. The dried powders were weighed on the scale KERN PLT 2000-3DM to accuracy to three decimal points. The weight of individual powders can be seen in Table 4.2.

Tab. 4.2 Quantities of powders for the fabrication of 200 grams of composition.

Powder	Weight
$BaCO_3$	150.478 g
ZrO_2	11.054 g
TiO_2	64.482 g
$CaCO_3$	13.467 g

4.2.2. Milling in horizontal mill

Powders are put into plastic container for mixing with 350 g of ZrO_2 milling media. There is also added 380 ml deionized water. Weight of milling media and quantity of deionized water is for fabrication of 200 g of resulting BCTZ powder. During first 6 hours of milling it is necessary to do control once per hour. The suspension must have a viscosity like "cream." The speed was adjusted to 27 rpm because the suspension must be mixed and if suspension is too thick we can add another 50 ml of deionized water after two hours of milling. Total

milling time was 24 hours. During milling in horizontal mill powders are mixed. Milling was performed on horizontal mill with milling stool type ML01.

Fig. 4.1 The container and milling media for horizontal mill.

Fig. 4.2 The containers with powders on horizontal mill.

After milling the suspension must be dried in a laboratory oven at 80 °C. The suspension was placed in large crystallization bowl during drying. Milling media were removed after drying. Dry powder was crushed in a mortar. After milling the powder was ready for calcination.

4.2.3. Calcination

Calcination occurs in a furnace NABERTHERM model HT 08/17 no. 203511. Powder was in crucible. Crucible is made of Al_2O_3. Calcination temperature was 1100 °C for 4 hours. The heating profile for the calcination is shown in Figure 4.3.

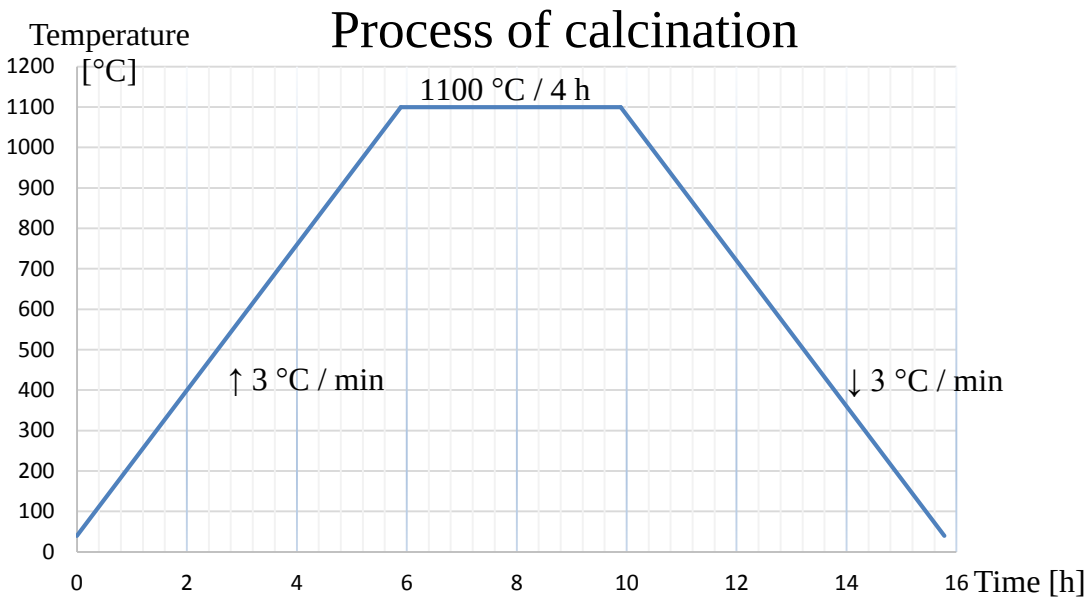

Fig. 4.3 The process of calcination.

4.2.4. Milling in planetary ball mill

Powder after calcination contains a large amount of agglomerates and large grains. Agglomerates are crushed in a mortar. Before milling binders to facilitate pressing were added. Used binders were Duramax B 1000 and B 1007. Weight of binders is calculated by the following formulas.

$$w_{B1000} = \frac{0.03}{0.55} w_{powder} \tag{6}$$

$$w_{B1007} = \frac{0.02}{0.37} w_{powder} \tag{7}$$

During milling in planetary ball mill other agglomerates are broken down, powder is mixed with the additives and grains after milling are finer. Powder was divided into four ZrO_2 bowls. Deionized water and ZrO_2 milling media were added to bowls. In each bowl was 100 g of powder, 250 ml of deionized water and 250 g of milling media. Milling was performed on Planetary ball mill FRITSCH pulverisette® type 05.102. Speed was adjusted to 224 rpm. Total milling time was 24 hours.

In planetary ball mill support plate rotates and mill bowls rotate in the opposite direction. The centrifugal forces act on powder and milling media in bowls.

After milling the suspension must be dried in a laboratory oven at 80 °C. Milling media were removed by sieves before drying. The suspension was placed in large crystallization bowl during drying. Dry powder was crushed in a mortar. The last step of fabrication of BCTZ

powder is sieving. Crushed powder was sieved through 300 μm stainless steel sieve Laboratory test sieve BS 410-1 serial no. 6293141.

Fig. 4.4 The bowl and milling media for planetary ball mill.

Fig. 4.5 The bowl with powder in planetary ball mill.

4.2.5. Pressing of samples

The samples were prepared by dry uniaxial pressing. A schematic diagram of uniaxial pressing can be seen in Figure 2.12. Pressing was conducted at room temperature. Green bodies with a diameter of 13 mm were compressed by pressure about 148 MPa.

4.2.6. Sintering

Sintering of green bodies occurs in a furnace NABERTHERM model HT 08/17 no. 203511.

Fig. 4.6 The furnace NABERTHERM.

The binders were removed by pre-sintering cycle. Sintering temperature was from 1300 °C to 1525 °C for 4 hours. The temperature profile of the sintering process with pre-sintering cycle can be seen in Figure 4.7. After sintering samples were polled at room temperature by DC high voltage power supply with maximum voltage of 30 kV. Samples were in container with silicon oil. And temperature was at room temperature. Poling conditions have big impact on the final properties especially on value d_{33}. Therefore, strict poling conditions must be adhered.

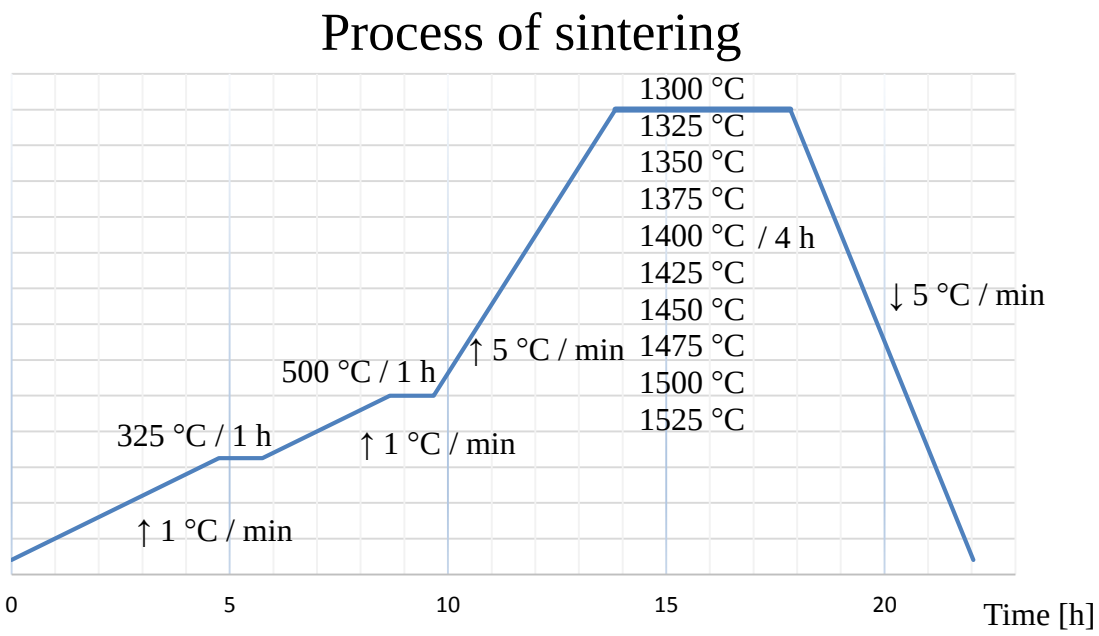

Fig. 4.7 The process of sintering of samples.

4.3. Preparation of samples for Microstructural Examination using SEM

SEM is an abbreviation for scanning electron microscope. Thanks to SEM, it is possible takes photos of microstructure and determines grain size.

The sintered discs were cut in half using a Struers Accutom-50 saw (Figure 4.8) with cutting disc M0D13. The prepared samples were sealed into the polystyrene (PS) for better handling during grinding and polishing.

Grinding and polishing were carried out on the Struers TegraPol-25 with additional head TegraForce-5 (Figure 4.9). The conditions and used grinding and polishing wheels can be seen in Table 4.3. The grinding was carried out on grinding wheel MD Piano 120 and with water as a wetting fluid, there was used a standard rotary grinding procedure. A climb rotary grinding procedure was used incorporating three cycles of polishing on polishing wheels MD Alegro Largo and MD Dac with TegraDoser DiaPro diamond suspensions of the appropriate granularity.

Tab. 4.3 Used grinding and polishing wheels and conditions of use.

Grinding or polishing wheel + diamond suspension	Granularity [µm]	Time [min]	Pressing force [N]	Speed [rpm]
MD Piano 120 (with water)	120	5	30	300
MD Alegro Largo + DiaPro 9 µm	9	10	25	150
MD Dac + DiaPro 3 µm	3	6	20	150
MD Dac + DiaPro 1 µm	1	6	15	150

After grinding and polishing the PS must be dissolved and samples removed. Polystyrene was dissolved by heating. Residues of PS on samples were dissolved in Xylene. The samples were washed in ethanol and deionized water. The samples were thermally etched for the observation of grain boundaries.

Fig. 4.8 StruersAccutom-50

Fig. 4.9 Struers TegraPol-25 with additional head TegraForce-5

4.4. Measurement of properties

The phase analysis was performed on the Automatic diffractometer SmartLab 3kW (Rigaku) in geometry Bragg-Brentano with linear encoder sensitive detector with CuK$\alpha_{1,2}$ radiation. In the analyzed powder was found phase composition, lattice parameters and theoretical density.

Density was determined using the Archimedes method in accordance with standard ČSN EN 623-2. Weight of samples and temperature of water were measured on the Analytical balance with density kit for measurement of density using the Archimedes method Mettler Toledo ME 104. Sample was at first wiped dry and weighed (m_1). The dried sample was immersed in a beaker with water and m_2 was measured, m_3 is the mass of again dried sample. Based on following formulas, we can calculate the absolute (8) and relative (9) density.

$$\rho_{abs} = \frac{m_1}{m_3 - m_2}\rho_{water}\ [kg\ m^{-3}] \tag{8}$$

$$\rho_{rel} = \frac{m_1}{m_3 - m_2}\frac{\rho_{water}}{\rho_{theretical}} * 100\ [\%] \tag{9}$$

Microstructure was evaluated on images from scanning electron microscope Zeiss ULTRA PLUS. Grain size was determined from the imagines using linear intercept method in accordance with standard ČSN EN 623-3. From each sample which was sintered at one of sintering temperatures were done several photographs from different locations. On these photographs was measured grain size. Values from different photographs were averaged and from the differences of values were established standard deviations.

On the samples, dimensions and weights before and after sintering were measured. From the measured values were calculated weight loss (10) and shrinkage (11) of samples during sintering. Values of weight loss and shrinkage are shown in percentages.

$$Weight\ loss = 100 - \frac{m_1}{m_{after\ sintering}} * 100\ [\%] \tag{10}$$

$$Shrinkage = 100 - \frac{Diameter_{after\ sintering}}{Diameter_{before\ sintering}} * 100\ [\%] \tag{11}$$

The values of d_{33} were measured at Berlincourt d_{33}-meter by quasi-static method at room temperature. The sample was clamped between two spikes, which vibrated at frequency 110 Hz. The pressure of spikes was 0.25 N. Sample was pressed and generated electric charge which was measured. The meter automatically calculated from the measured values value of d_{33}.

5. Results and discussion

The XRD analysis has revealed the lattice parameters (Tab 5.1). Values of the lattice parameters shown that it was achieved single phase composition with a tetragonal structure which corresponds with the literature [5]. XRD analysis demonstrated the tetragonal structure as can be seen in figure 5.1 which is example of the XRD trace for sintering temperature 1325 °C. For other sintering temperatures are the XRD traces very similar and in a common plot peaks would be overlayed. The theoretical density ($\rho_{theoretical}$ = 5.7298 g·cm^{-3}) was calculated from these parameters (Tab 5.1).

Tab 5.1 Average values of the lattice parameters.

a Å	b Å	c Å	α o	β o	γ o
4.0082	4.0082	4.0160	90	90	90

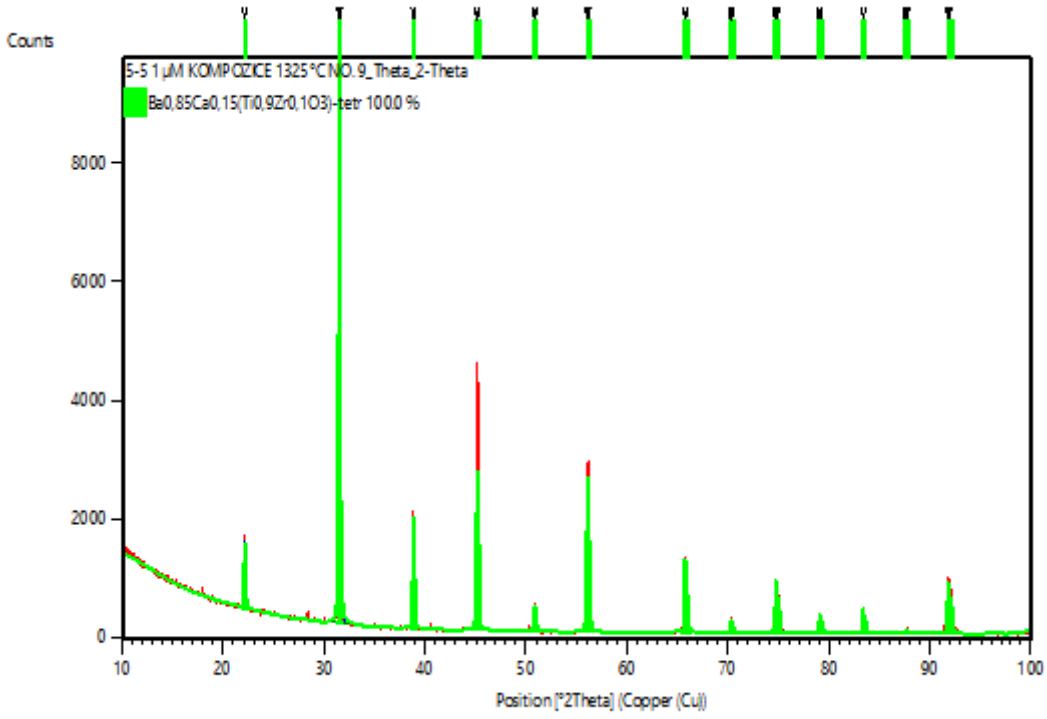

Fig. 5.1 The XRD trace for sintering temperature 1325 °C.

The relative density was calculated from theoretical density (9). A plot of the dependence of density on sintering temperature can be seen in Figure 5.2.

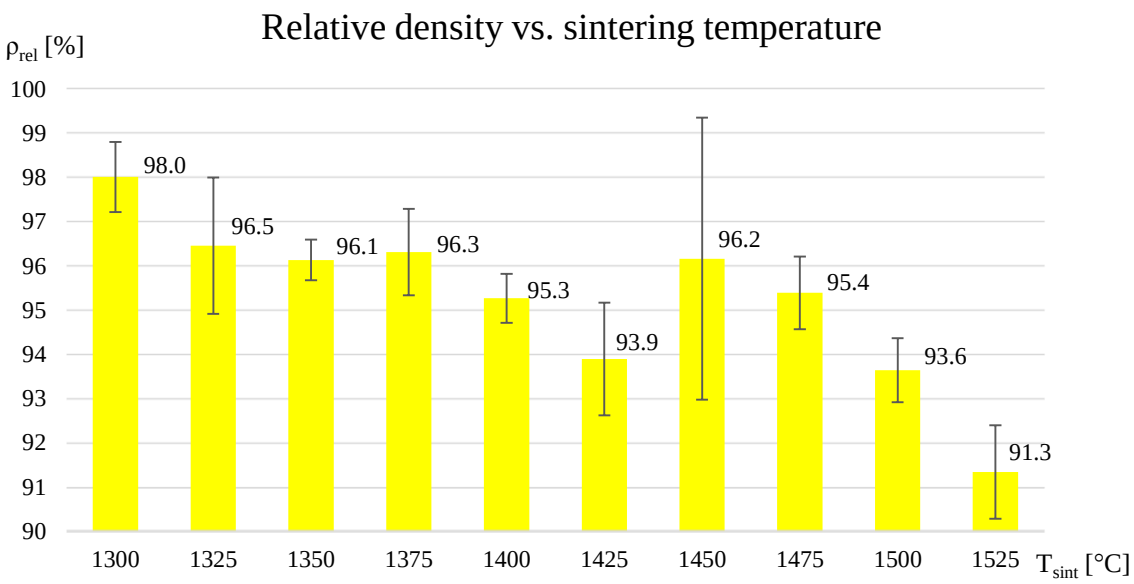

Fig. 5.2 Plot of dependence of density on sintering temperature.

Standard deviations are about 2 %, except for the samples sintered at 1450 °C, where a higher value was measured. Assuming that the true value lies in the indicated range it can be said that the relative density is about 96 %. It is in contradiction with the literature [23], where authors claimed that the density should increase with increasing sintering temperature until T_{sint} = 1450 °C. In accordance with the literature [23] is the maximum relative density of about 96 % and a decrease of the relative density for sintering temperatures above 1450 °C.

From the weights and dimensions of the samples the shrinkage (11) and weight losses (10) during sintering were calculated.

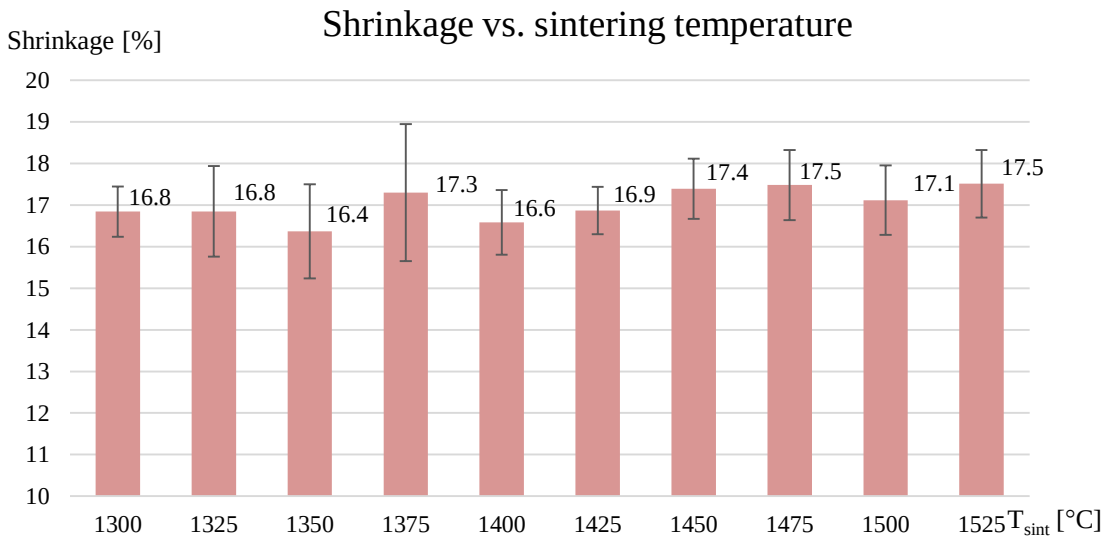

Fig. 5.3 Plot of dependence of shrinkage on sintering temperature.

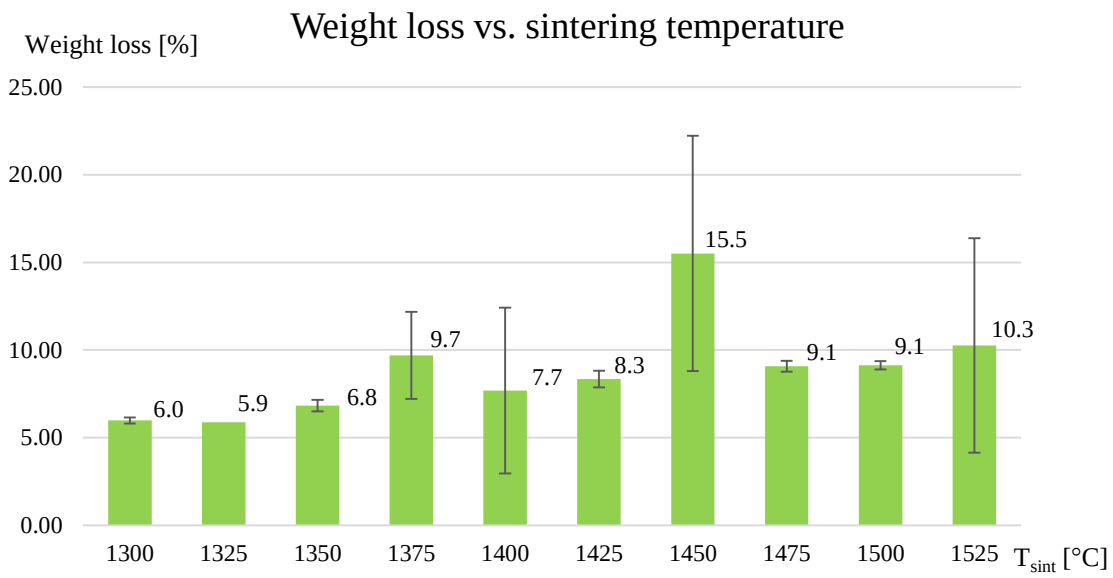

Fig. 5.4 Plot of dependence of weight losses on sintering temperature.

In Figure 5.3 can be seen shrinkage around 17 % at all temperatures. In Figure 5.4 can be seen gradually increasing the value of weight loss from 5.98 % to 10.26 % with increasing sintering temperature. The values of weight loss at temperatures 1375 °C and 1450 °C don't fit into the gradually increasing profile, but standard deviations of these values are high, therefore, they can be incorporated to the gradually increasing profile.

5.1. Microstructure

Microstructure was observed using SEM. In Figure 5.5 can be seen images from SEM for the different sintering temperatures.

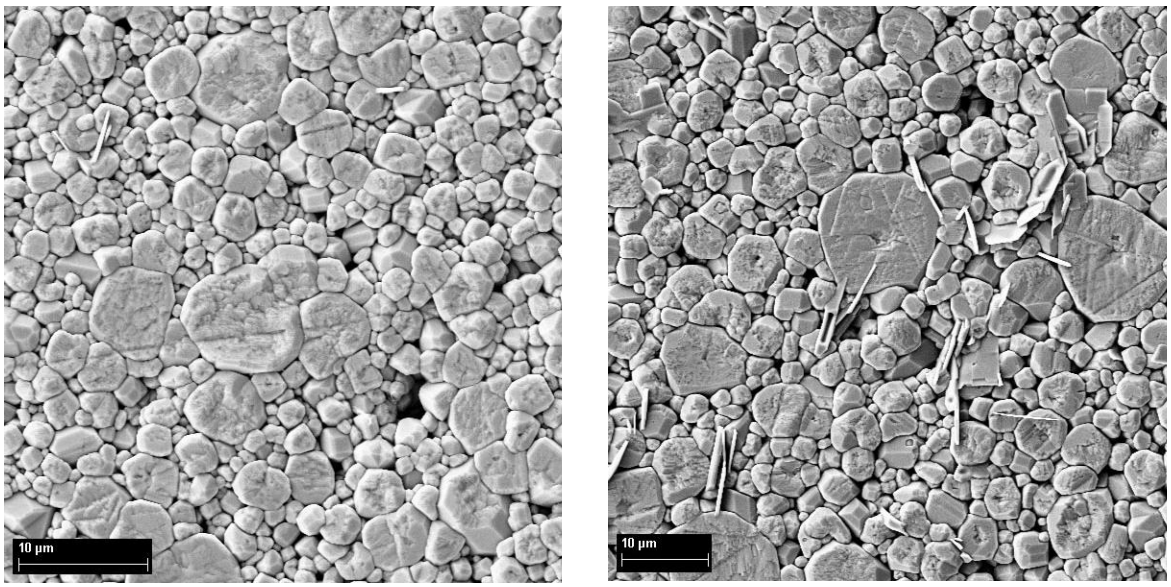

a) T_{sint} = 1300 °C

b) T_{sint} = 1325 °C

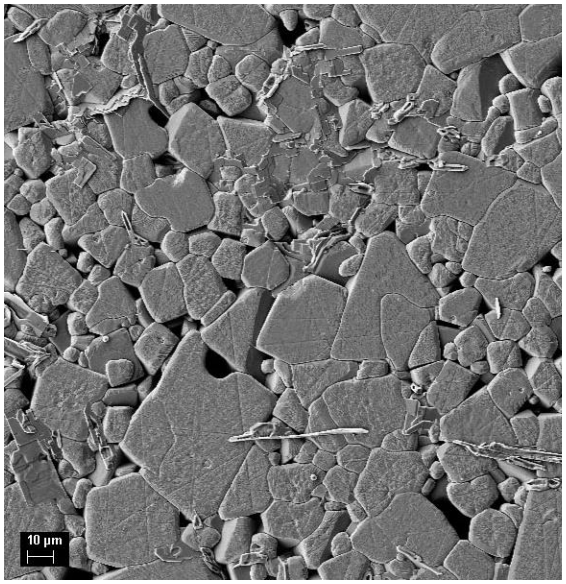

c) T_{sint} = 1350 °C

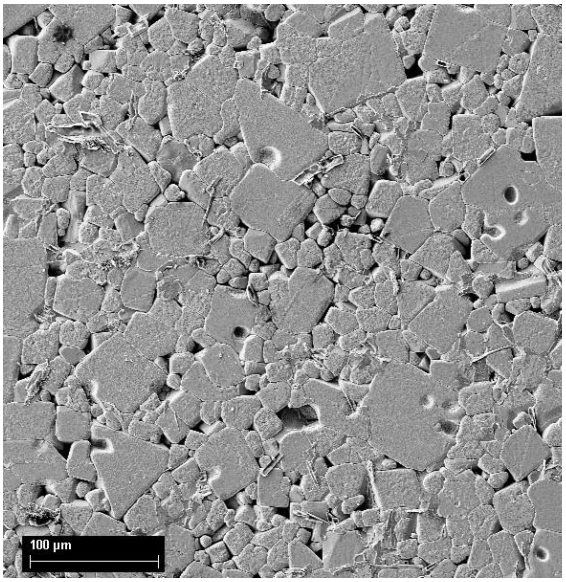

d) T_{sint} = 1375 °C

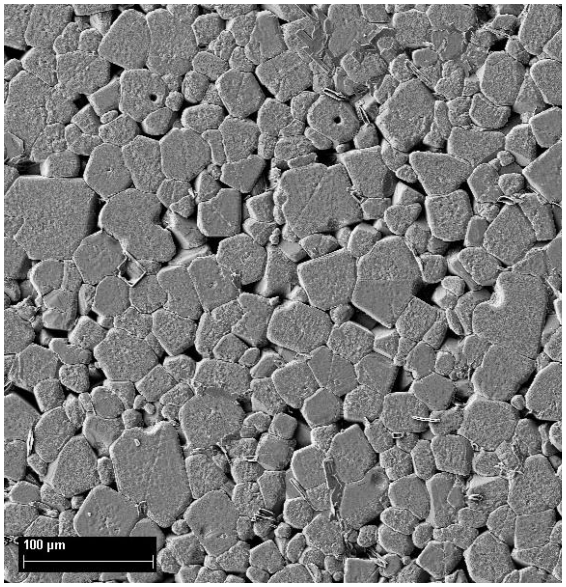

e) T_{sint} = 1400 °C

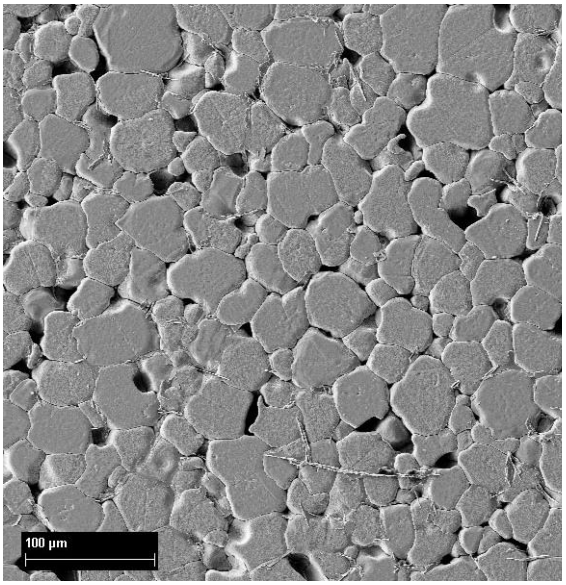

f) T_{sint} = 1425 °C

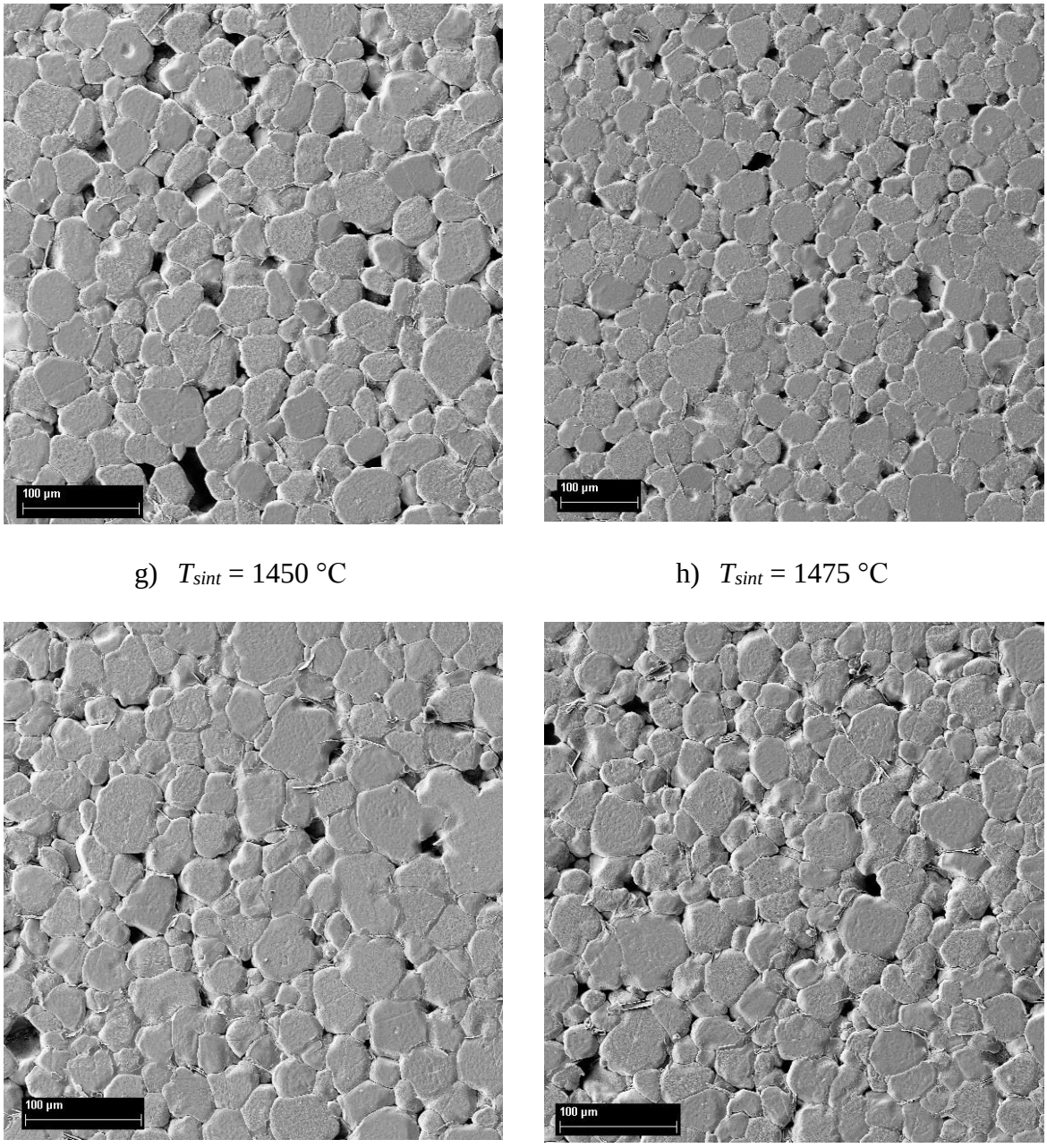

g) T_{sint} = 1450 °C

h) T_{sint} = 1475 °C

i) T_{sint} = 1500°C

j) T_{sint} = 1525 °C

Fig 5.5 The microstructure of samples at different sintering temperatures (T_{sint}).

Images show that porosity is decreasing with increasing of sintering temperature which corresponds with the literature [23]. The values of grain size depending on sintering temperature can be seen in Figure 5.6. The grain size of samples which were sintered at low temperature (1300 °C) is under 10 µm and increases with increasing sintering temperature. This is consistent with the literature [23]. Grain size increases to T_{sint} = 1400 °C. Above this temperature is almost constant until last value, there is a small drop. But this value has big standard deviation from this we can conclude that the value falls to the almost constant course. Constant progression above T_{sint} = 1400 °C is also mentioned in the literature [22]. Also worth pointing out that the grain size in samples sintered at temperatures 1400 °C

and below have large range of grain sizes – some very large, some small as can be seen in figures 5.5 a) – e).

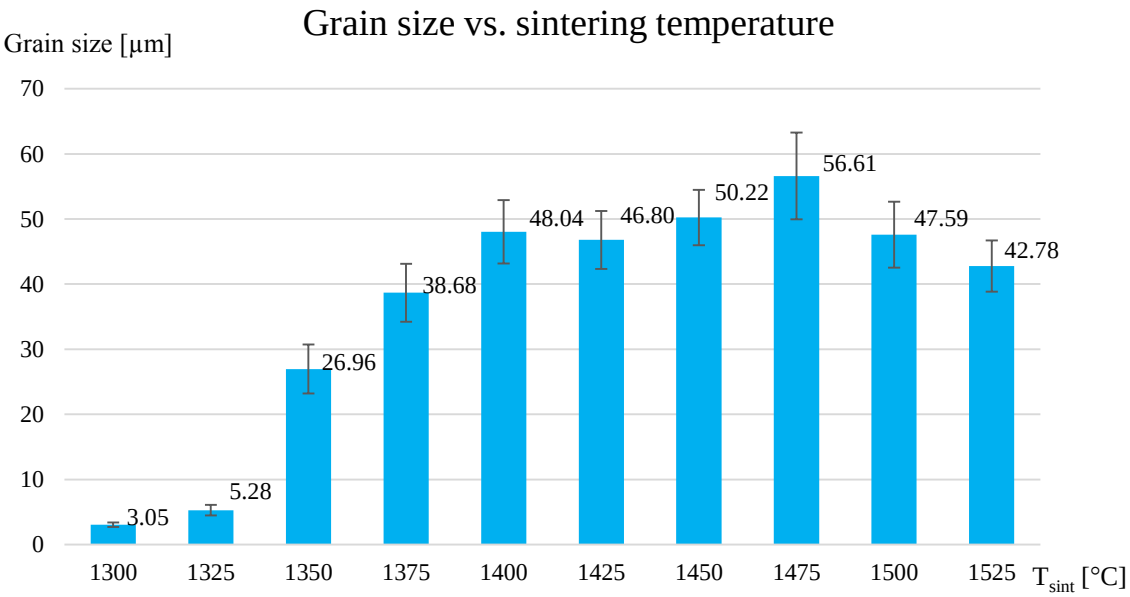

Fig 5.6 Plot of dependence of grain size on sintering temperature.

5.2. Electrical properties

Measured values of d_{33} can be seen in Figure 5.7. The plot shows d_{33} increasing with increasing sintering temperature to T_{sint} = 1425 °C followed by drop and the further course is almost constant which is consistent with the literature [22].

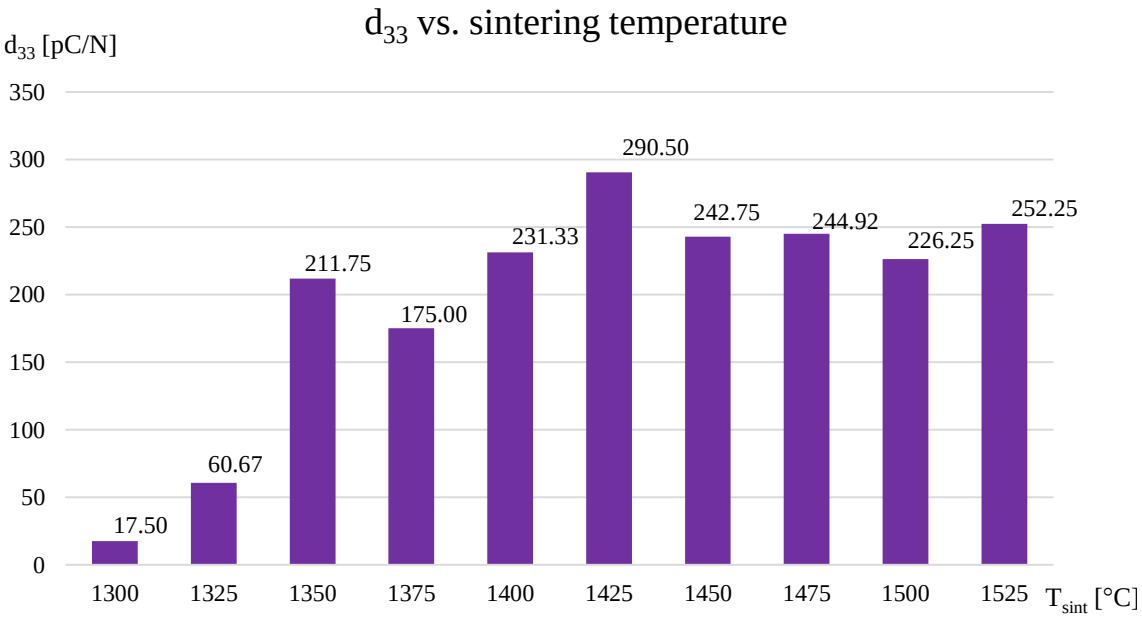

Fig 5.7 Plot of dependence of d_{33} on sintering temperature.

The high d_{33} published in the literature [5] were not achieved. The reasons may be different calcination temperature or poling conditions. Especially poling conditions have a large influence as mentioned above. Another reason may be there are no measurement conditions mentioned in the literature [5]. Value of d_{33} is dependent on place of measurement, therefore, it is necessary to do measuring at several places on sample. Value of d_{33} can't be compared with literature [5] because in this literature poling conditions aren't mentioned and measurement conditions aren't mentioned too.

According to the literature [4], density and grain size have an important effect on the piezoelectric constant, but grain size affects d_{33} more markedly than density. This also demonstrates our progress. You can compare effect of grain size and relative density to d_{33} in Figure 5.8. The relative density is highest at low sintering temperature but grain size at low sintering temperature is very small and d_{33} is small too. Comparing the d_{33}, density and grain size for the sample sintered at 1350C one can say that a grain size of at least 25 microns is needed for a reasonable value of d_{33}. At T_{sint} = 1525 °C we can see relatively high value of d_{33} but relative density is the smallest, we can conclude grain size lies at the upper limit of the standard deviation. Because of this we can considered as constant the plot of dependence grain size on sintering temperature above T_{sint} = 1400 °C.

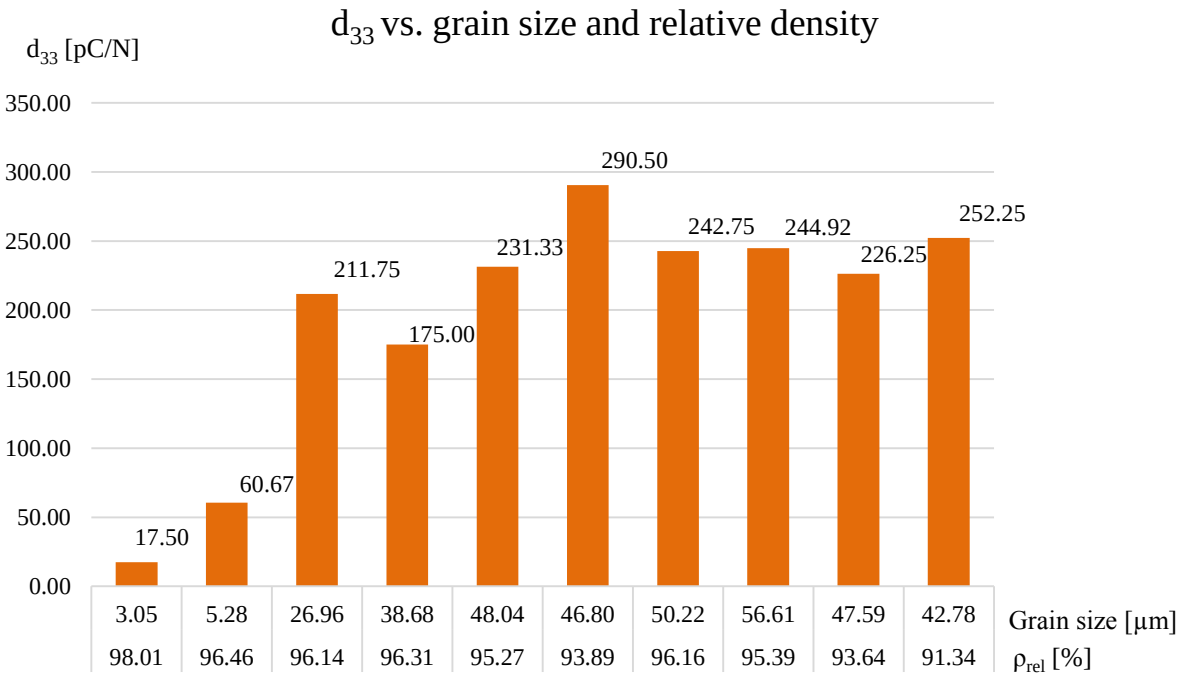

Fig 5.8 Plot of dependence of d_{33} on grain size and relative density.

6. Conclusions

In the literature review was prepared treatise about basic principles, properties, history, fabrication and applications of leaded and lead-free piezoelectric ceramics.

In the experimental approach the fabrication of lead-free piezoceramic BCTZ powders, preparation of sintered samples from this ceramic powder and measurement of the physical and piezoelectric properties were described.

The X-ray diffraction analysis showed samples had single phase structure. The best electrical properties were measured at a sintering temperature of 1425 °C, where d_{33} = 290.5 pC/N, average value of grain size is 46.8 μm and relative density is 93.9 %.

BCTZ lead-free piezoceramics are promising for the future, but further research and development in this field is necessary. One potential line of research could be to investigate doping the BCTZ composition with other elements or other compositions.

Aspects of this work have contributed to a scientific publication to be presented at the International Symposium on the Applications of Ferroelectrics (ISAF), Singapore, 24.-27. May 2015, and a copy of the paper is given in the Appendix.

7. References

[1] MOULSON, A. and J. HERBERT. *Electroceramics: materials, properties, applications*. 2nd ed. New York: Wiley, 2003, 557 p. ISBN 04-714-9748-7

[2] ERHART J. Piezoelektrické "chytré" materiály pro elektrotechniku: PZT keramika. *Elektro*, 2002, no.11, pp. 4-7.

[3] QIAO, S., J. WU, B. WU, B. ZHANG, D. XIAO and J. ZHU. Effect of Ba0.85Ca0.15Ti0.90Zr0.10O3 content on the microstructure and electrical properties of Bi0.51(Na0.82K0.18) 0.50TiO3 ceramics. *Ceramics International*. 2012, vol. 38, issue 6, pp. 4845-4851.

[4] WANG, P., Y. LI and Y. LU. Enhanced piezoelectric properties of (Ba0.85Ca0.15)(Ti0.9Zr0.1)O3 lead-free ceramics by optimizing calcination and sintering temperature. *Journal of the European Ceramic Society*. 2011, vol. 31, issue 11, pp. 2005-2012.

[5] LIU, W. and X. REN. Large Piezoelectric Effect in Pb-Free Ceramics. *Physical Review Letters*. 2009, vol. 103, issue 25.

[6] KOUKOLÍK, V. *Využití piezolektrického jevu v praxi.* Plzeň: Západočeská univerzita v Plzni, Fakulta elektrotechnická, 2013. 77 p. Thesis Supervisor Doc. Ing. Eva Kučerová, CSc.

[7] PIEZOELECTRICITY. APC International, Ltd.. [online]. [cit. 2015-01-14]. Available from: https://www.americanpiezo.com/knowledge-center/piezo-theory/ piezoelectricity.html

[8] SAFARI, A. and E. K. AKDOGAN. *Piezoelectric and acoustic materials for transducer applications*. New York: Springer, 2008. ISBN 0387765387.

[9] HANUS, J. *Využití piezo-materiálu pro získávání elektrické energie z vibrací.* Brno: Vysoké učení technické v Brně, Fakulta strojního inženýrství, 2009. 63 p. Thesis Supervisor Ing. Zdeněk Hadaš, Ph.D.

[10] LEDOUX, A. *Therory of Piezoelectric Materials and Their Applications in Civil Engineering.* Massachussets institute of technology, Department of Civil and Environmental Engineering, 2011. 49 p. Thesis Supervisor Prof. Jerome Connor

[11] CALLISTER, W. D. and D. G. RETHWISCH. *Materials science and engineering: an introduction*. 8th ed. /. Hoboken, NJ: John Wiley&Sons, 2010, 885 p. ISBN 0470419970.

[12] ASKELAND, D. R., P. P. FULAY and W. J. WRIGHT. *The science and engineering of materials*. 6th ed. Stamford, CT: Cengage Learning, 2011, 921 p. ISBN 0495296023.

[13] PLASS, P. *Piezo Legs motor v lékařské aplikaci*. Brno: Vysoké učení technické v Brně, Fakulta elektrotechniky a komunikačních technologií, 2009. 66 p. Thesis Supervisor Ing. Tomáš Ondrák.

[14] SKÁCEL, V., J. FIEDLEROVÁ a K. NEJEZCHLEB. Keramické materiály a jejich použití v elektrotechnice. *T-ceram.com* [online]. [cit. 2014-12-05]. Available from: http://www.t-ceram.com/CSVTS-2006.pdf

[15] BENAM, M. R. Investigation the dielectrical and electromechanical properties of PZT thin films. *International Journal of Engineering Research and Applications.* 2013, vol. 3, issue 2, pp. 680-682. ISSN: 2248-9622

[16] Proces výroby piezokeramiky. *CeramTech.* [online]. [cit. 2015-01-26]. Available from: *http://www.ceramtec.cz/ceramic-materials/piezo-ceramics/manufacturing-process/*

[17] Wilkinson, A. P.. *Solid State Synthetic Methods* [online]. 2001 [cit. 2015-01-22]. Available from: http://ww2.chemistry.gatech.edu/class/6182/wilkinson/solid-state.pdf

[18] TRESSLER, J. F., S. ALKOY, A. DOGAN and R. E. NEWNHAM. Functional composites for sensors, actuators and transducers. *Composites Part A: Applied Science and Manufacturing*. 1999, vol. 30, issue 4, pp. 477-482.

[19] BADAPANDA, T., S. VENKATESAN, S. PANIGRAHI and P. KUMAR. Structure and dielectric properties of bismuth sodium titanate ceramic prepared by auto-combustion technique: Phase transition, sintering and property enhancement. *Processing and Application of Ceramics*. 2013, vol. 7, issue 3, pp. 135-141.

[20] WANG, K. and J.-F. LI. (K, Na)NbO3-based lead-free piezoceramics: Phase transition, sintering and property enhancement. *Journal of Advanced Ceramics*. 2012, vol. 1, issue 1, pp. 24-37.

[21] ULLAH, A., Ch. W. AHN, A. HUSSAIN and I. W. KIM. The effects of sintering temperatures on dielectric, ferroelectric and electricfield - induced strain of lead-free Bi0.5(Na0.78K0.22)0.5TiO3 piezoelectric ceramics synthesized by the sol–gel technique. *Current Applied Physics*. 2010, vol. 10, issue 6, pp. 1367-1371.

[22] WU, J., D. XIAO, B. WU, W. WU, J. ZHU, Z. YANG and J. WANG. Sintering temperature – induced electrical properties of (Ba0.90Ca0.10)(Ti0.85Zr0.15)O3 lead-free ceramics. *Materials Research Bulletin*. 2012, vol. 47, issue 5, pp. 1281-1284.

[23] LI, W., Z. XU, R. CHU, P. FU and G. ZANG. High piezoelectric d33 coefficient of lead-free (Ba0.93Ca0.07)(Ti0.95Zr0.05)O3 ceramics sintered at optimal temperature. *Materials Science and Engineering: B*. 2011, vol. 176, issue 1, pp. 65-67

Appendix

The published paper

Phase Transitions and Dielectric, Ferroelectric and Piezoelectric Properties of $Bi_{0.5}(Na_{0.82}K_{0.18})_{0.5}TiO_3$-doped $(Ba_{0.85}Ca_{0.15})(Zr_{0.1}Ti_{0.9})O_3$ Ceramics

Yang Bai, Ales Matousek, Pavel Tofel, Bo Nan, Vijay Bijalwan, Michael Kral, Hana Hughes and Tim W. Button
Central European Institute of Technology - CEITEC
Brno 616 00, Czech Republic
yang.bai@ceitec.vutbr.cz

Yang Bai, Hojat Pooladvand and Tim W. Button
School of Metallurgy and Materials
University of Birmingham – UoB
Birmingham B15 2TT, United Kingdom
t.w.button@bham.ac.uk

Abstract—*This paper reports an investigation of $(Ba_{0.85}Ca_{0.15})(Zr_{0.1}Ti_{0.9})O_3$ (50BCZT) piezoelectric ceramics doped with $Bi_{0.5}(Na_{0.82}K_{0.18})_{0.5}TiO_3$ (18BNKT). For compositions between 1-5 wt% 18BNKT, a perovskite phase was observed in the sintered ceramics, with d_{33} values of approximately 370 pC/N measured at room temperature, which is about 80 % of that of pure 50BCZT. Also, the doped materials exhibit a remanent polarization of 2-5 $\mu C/cm^2$ at temperatures above the Curie temperature (> 90 °C) of the pure 50BCZT composition. This research shows a promising route to improve the working temperature range whilst maintain good piezoelectric properties of the 50BCZT ceramics.*

Keywords—*piezoelectric, BCZT, BNKT, Curie temperature*

I. INTRODUCTION

Driven by impending environmental legislation [1], there is now an urgent need to develop environmentally friendly piezoelectrics. The reason is that lead (Pb), a highly toxic element, is widely used in a range of piezoelectric ceramic compositions which have dominated the materials market of important sensors, actuators, transducers and energy harvesters. Lead zirconate titanate (PZT, $PbZr_xTi_{1-x}O_3$) is a typical representative which is targeted to be replaced by lead-free compositions. The lead-free perovskite solid-solution, $(1-x)(Ba_{0.7}Ca_{0.3})TiO_3$-$xBa(Zr_{0.2}Ti_{0.8})O_3$ ((1-x)BZT-xBCT), has been the subject of much research, with work on bulk ceramics [2], thin/thick-films [3, 4] and composites [5] having been reported. BZT-BCT has become significant among the families of lead-free piezoelectric materials showing promise to replace conventional PZT, due to its potential for exhibiting piezoelectric properties which are comparable to those of 'soft' PZT (e.g. d_{33} > 600 pC/N, k_p > 0.5), especially for the composition of 0.5BZT-0.5BCT (alternatively expressed as $(Ba_{0.85}Ca_{0.15})(Zr_{0.1}Ti_{0.9})O_3$). It has been reported [2], that this centre composition of the BZT-BCT pseudo-phase diagram is associated with a strongly curved morphotropic phase boundary (MPB) at approximately room temperature, which is probably at least partly responsible for the excellent piezoelectric properties. However, the low Curie temperature (T_c) of about 90 °C of 0.5BZT-0.5BCT considerably restricts its application above room temperature.

On the contrary, other lead-free systems exhibit much higher Curie temperatures, but with piezoelectric properties which are only about half

of those of 'soft' PZT [6]. In particular, the $Bi_{0.5}(Na_{1-x}K_x)_{0.5}TiO_3$ lead-free system is reported to have a T_c of approximately 300 °C, and a de-poling temperature (T_d) of nearly 200 °C around its own MPB ($0.16 < x < 0.2$). However, the reported d_{33} and k_p values are < 200 pC/N and < 0.5 respectively [6]. One route to investigate enhancing the T_c of 0.5BZT-0.5BCT whilst minimizing any deterioration in its piezoelectric properties would be through a combination of 0.5BZT-0.5BCT and $Bi_{0.5}(Na_{1-x}K_x)_{0.5}TiO_3$. Studies have been reported where 0.5BZT-0.5BCT has been added as a dopant to $Bi_{0.5}(Na_{0.82}K_{0.18})_{0.5}TiO_3$ (18BNKT) [7]. However, it has been found that both the piezoelectric properties (e.g. d_{33}, k_p) and the T_c/T_d are approximately independent of the 0.5BZT-0.5BCT doping, with the 18BNKT always appearing to dominate the performance of the system. This paper presents the research of an alternative approach, where 18BNKT is doped into 0.5BZT-0.5BCT.

II. Experimental

The compositions of $(Ba_{0.85}Ca_{0.15})(Zr_{0.1}Ti_{0.9})O_3$ (0.5BZT-0.5BCT) and $Bi_{0.5}(Na_{0.82}K_{0.18})_{0.5}TiO_3$ (18BNKT) were prepared separately via solid-state reaction, calcined at 1100 °C and 750 °C respectively. The starting oxides were $BaCO_3$ (> 99.5 %, Dakram, UK), $CaCO_3$ (PA, Lachner, Czech Republic), ZrO_2 (> 99.5 %, Dakram, UK) and TiO_2 (> 99.5 %, Dakram UK) for the 0.5BZT-0.5BCT, and Bi_2O_3 (PA, Dakram, UK), Na_2CO_3 (PA, Penta, Czech Republic), K_2CO_3 (PA, Penta, Czech Republic) and TiO_2 for the 18BNKT. 0.5 mol% excess Bi_2O_3 was added to the 18BNKT composition in order to compensate for Bi loss during high temperature sintering. Subsequently, doped compositions were made by adding calcined 18BNKT powder into the calcined 0.5BZT-0.5BCT powder at concentrations of 1, 3 and 5 wt%, but without re-calcination. The combined powders were then mixed with a PVA binder (5 wt% DURAMAX B-1000 + 5 wt% DURAMAX B-1007, Chesham Chemicals Ltd., UK) and pressed into discs by uniaxial pressing, followed by sintering at temperatures between 1250-1500 °C for 4 hours. The density of the sintered ceramics were calculated by the Archimedes method, and then expressed as a percentage of the theoretical density, this ratio being defined as the relative density. The sintered samples with sputtered Au-Cr electrodes (K575X, Emitech, UK) or printed and fired Ag electrodes (Gwent Group, UK) were tested on a piezoelectric

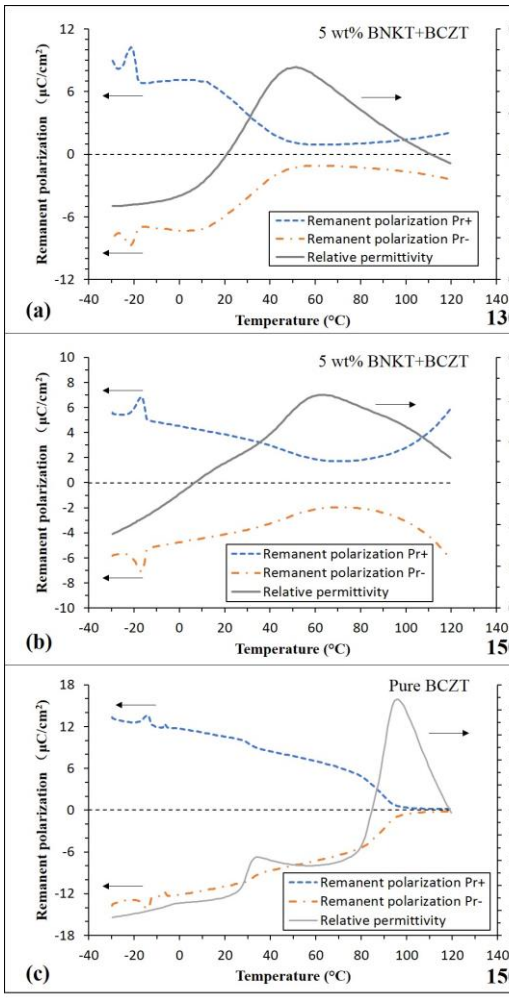

Fig. 1. Dependence of remanent polarization and relative permittivity on temperature for the 5 wt% BNKT+BCZT samples sintered at (a) 1300 ℃ and (b) 1500 ℃, and (c) the pure BCZT sample sintered at 1500 ℃.

evaluating system (AixPES, Aixacct, Germany) at temperatures in the range of -30 to 120 °C. In addition, the samples were poled with 3 kV/mm electric field for 10 minutes at room temperature in silicone oil and subsequently characterised at room temperature on an impedance analyzer (4294A, Agilent, USA) and a Berlincourt d_{33}-meter (YE2730A, Sinoceera, China). The relative permittivity (ε_r), piezoelectric coefficient (d_{33}), and polarization-electric field (P-E) and strain-electric field (S-E) hysteresis loops were then obtained. X-ray diffraction (XRD, SmartLab, Rigaku, Japan) was used for structural characterization. Polished samples were thermally etched at 100 °C below the sintering temperatures and then observed using scanning electron microscopy (SEM, Ultra Plus, Zeiss, USA). Pure 18BNKT and 0.5BZT-0.5BCT

ceramics were also fabricated and characterized with the same processes, providing base line references to the doped compositions. In this paper, the doped samples are abbreviated to x wt% BNKT+BCZT (x=1, 3, 5), whilst the pure 18BNKT and 0.5BZT-0.5BCT samples are further shortened to BNKT and BCZT respectively for ease of repetition.

III. Results and Discussions

A. Phase Transitions and Ferroelectric Properties

The variations of remanent polarization (Pr+ and Pr-) and relative permittivity (ε_r) with temperature for the 5 wt% BNKT+BCZT samples sintered at 1300 °C and 1500 °C, and the pure BCZT samples sintered at 1500 °C, are shown in Fig. 1. It can be seen that the pure BCZT exhibited 3 peaks in the relative permittivity in the range of -30 °C to 120 °C, at around 0 °C, 30 °C and 90 °C respectively (Fig. 1 (c)). This may imply 3 corresponding phase transitions, including 2 ferroelectric-ferroelectric and 1 ferroelectric-paraelectric transitions [8]. The transition around 90 °C is indicative of the T_c, where the remanent polarization dropped to zero as the structure became cubic. Below the T_c, the remanent polarization gradually decreased with the increase of temperature, and two gradient changes are observed corresponding to the other phase transition temperatures. However, for the samples doped with 5 wt% BNKT, a very broad peak of ε_r with temperature was observed (Fig. 1 (a) and (b)), which may imply a rather wide phase transition temperature range. This phenomenon was similar to that observed for pure BNKT [7] but which was observed at a much higher temperature (peak at about 300 °C). Interestingly, compared to the pure BCZT sample where the remanent polarization completely disappeared above T_c, the remanent polarizations of the 5 wt% BNKT+BCZT samples reached a minimum at a temperature corresponding to the maximum in ε_r, but never actually reached zero. Then, as the temperature was increased above approximately 70 °C an increase in remanent polarization was observed (Fig. 1 (a) and (b)), especially for the sample sintered at 1500 °C. This indicates a possibility of maintaining piezoelectric response for the sample in the full range of -30 °C to 120 °C. The remanent polarizations exhibited at lower temperatures in Fig. 1 (a) and (b) might be contributed by the BCZT composition, while those at higher temperatures might come from the BNKT dopant.

The P-E and S-E loops of the 5 wt% BNKT+BCZT sample sintered at 1500 °C and measured at different temperatures are shown in Fig. 2. Spontaneous and remanent polarization values in the ranges of 5-10 μC/cm^2 and 2-5 μC/cm^2, respectively were measured for temperatures between 20 and 110 °C. Between 20 and 60 °C (Fig. 2 (a) to (c)), both the spontaneous and remanent polarizations decreased with increased temperature. However, at temperatures from 80 °C (Fig. 2 (d)) and beyond the spontaneous polarization retained approximately the same value while the remanent polarization

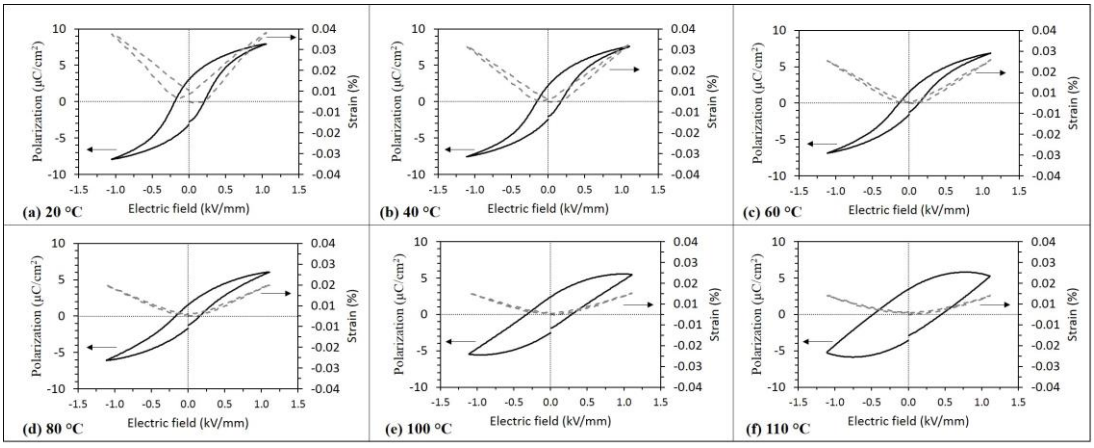

Fig. 2. Dependence of polarization and strain on electric field measured at (a) 20 ℃ (b) 40 ℃ (c) 60 ℃ (d) 80 ℃ (e) 100 ℃ and (f) 110 ℃ for the 5 wt% BNKT+BCZT sample sintered at 1500 ℃.

increased with increasing temperature. It can also been seen that in the temperature range 20-60 ℃ (Fig. 2 (a) to (c)) the sample became ‘‘softer’’ as the coercive electric field was reduced, however,

as the temperature was increased further (from Fig. 2 (d)) the coercive electric field was increased. The reported coercive electric field values for pure 0.5BZT-0.5BCT [8] are much smaller than for 18BNKT [7] (about 0.5 and 1.7 kV/mm respectively). Therefore, in the temperature range 80-110 °C (Fig. 2 (d) to (f)) there is an indication that the properties were becoming more like BNKT as the contribution from BCZT diminished. In addition, although the polarization varied irregularly as discussed above, the maximum strain of the sample, and the strain hysteresis, decreased with increasing temperature over the entire measured range, indicating a deterioration of the actuating properties, with the data between 80-110 °C being more indicative of electrostrictive behaviour.

The XRD patterns of the individually calcined BNKT and BCZT powders as well as the 5 wt% BNKT+BCZT ceramic sample sintered at 1500 °C are shown in Fig. 3. Both the individually calcined BNKT and BCZT powders formed single phase perovskite structures during calcination (Fig. 3 a and b). The sintered doped material also appears to form a single phase perovskite phase (Fig. 3 c). However, as the concentration of the BNKT dopant was very low, any secondary phases may be below the detection limit of the XRD system.

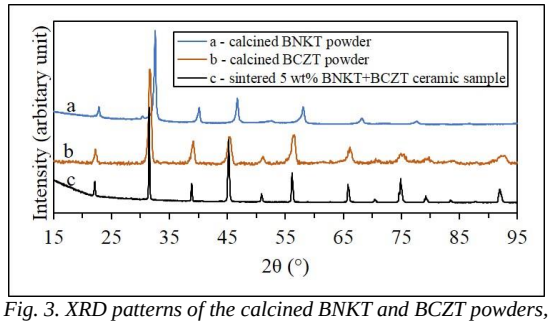

Fig. 3. XRD patterns of the calcined BNKT and BCZT powders, and the 5 wt% BNKT+BCZT ceramic sample sintered at 1500 °C.

SEM images of polished and thermal-etched surfaces of the 5 wt% BNKT+BCZT samples sintered at temperatures from 1300 °C to 1500 °C are shown in Fig. 4. The sample sintered at 1300 °C, exhibited an irregular grain size from a few microns to 30 µm (Fig. 4 (a)). The grain size of the samples sintered at 1400 °C and 1500 °C (Fig. 4 (b) and (c)) were more regular, being in the range 20-30 µm and 40-50 µm, respectively, the overall grain size increasing with increased sintering temperature.

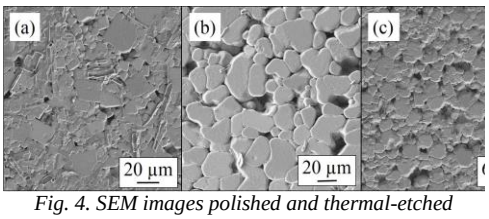

Fig. 4. SEM images polished and thermal-etched surfaces of the 5 wt% BNKT+BCZT samples sintered at (a) 1300 °C (b) 1400 °C (c) 1500 °C.

B. Physical, dielectric and Piezoelectric Properties

The density, relative permittivity and d_{33} values of the 1 wt%, 3 wt% and 5 wt% BNKT+BCZT samples sintered at different temperatures and measured at room temperature are shown in Fig. 5. All of the samples sintered below 1500 °C obtained densities > 90 % (Fig. 5 (a)). However, the densities tended to decrease with increasing sintering temperature, which might be due to Bi loss at high temperatures. The 5 wt% BNKT+BCZT samples sintered at 1500 °C exhibited a significantly lower density compared to those of other compositions and sintering temperatures. The variation in ε_r was quite different to that of the density. With increased sintering temperature, the 1 wt% BNKT+BCZT samples tended to exhibit increased ε_r. In comparison, both the 3 wt% and 5 wt% BNKT+BCZT samples showed peaks in the ε_r data at sintering temperatures of 1400 and 1300 °C respectively (Fig. 5 (b)). Among the three compositions, the largest ε_r value was obtained on the 5 wt% BNKT+BCZT samples sintered at and below 1450 °C and on the 1 wt% BNKT+BCZT samples sintered at 1500 °C. The trend in d_{33} values was much more consistent compared to the density and ε_r. For all the compositions, d_{33} values increased with sintering temperature (Fig. 5 (c)). However, the doping of BNKT had a considerable deteriorating effect with maximum d_{33} values reducing from 370 to 100 pC/N as the dopant concentration increased from 1 to 5 wt% BNKT. Compared to pure BCZT (optimum ε_r of 1800 and d_{33} of about 460 pC/N) and pure BNKT (optimum ε_r of 1400 and d_{33} of 165 pC/N, based on samples fabricated and measured in our own laboratories using the same methods described here), the 1 wt% BNKT+BCZT samples sintered at 1500 °C achieved an ε_r value of about 3600 and optimum d_{33} of 370 pC/N. The ε_r value was 2-2.5 times, and the d_{33} value reached 80 % and 280 % respectively, of those exhibited by the pure BCZT and BNKT ceramics. Such values are much better than those reported for BNKT+BCZT ceramics where the BCZT is the minor dopant [7]. This may be due to the better piezoelectric properties in pure BCZT compared to those in the pure BNKT [2, 6, 7].

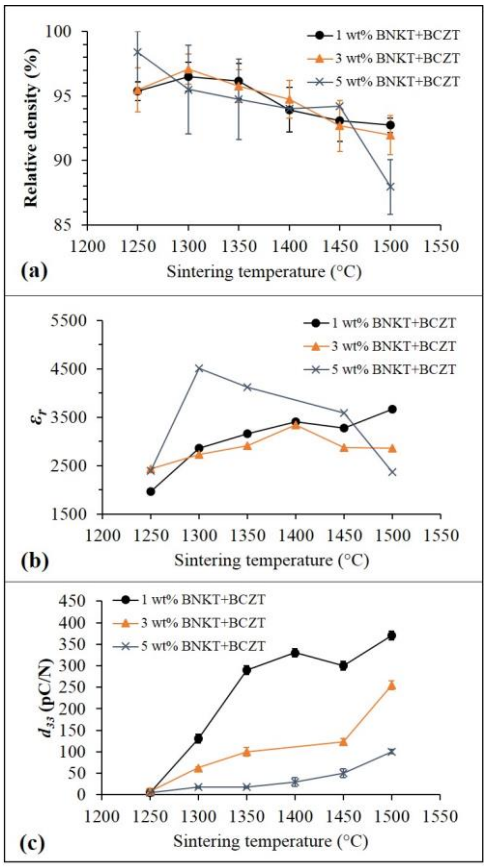

Fig. 5. Dependence of (a) relative density (b) ε_r and (c) d_{33} on sintering temperature for the 1 wt%, 3 wt% and 5 wt% BNKT+BCZT samples and measured at room temperature.

IV. Conclusions

Sintered ceramics with compositions of 1, 3 and 5 wt% $Bi_{0.5}(Na_{0.82}K_{0.18})_{0.5}TiO_3$ doped $(Ba_{0.85}Ca_{0.15})(Zr_{0.1}Ti_{0.9})O_3$ have been fabricated and characterized. Perovskite ferroelectric phases have been formed by the reaction of the dopant and matrix during sintering. At room temperature, the 1 wt% doped samples have exhibited comparable functional properties to the samples made from the pure matrix composition and much better than those of pure dopant composition. Also, in the doped samples, ferroelectric behaviour, exemplified by the remanent polarization, is observed at temperatures above the Curie temperature of the matrix composition. Although an increase in Curie temperature has not yet been clearly defined, the doping has shown a definite effect of enhancing the working temperature of the $(Ba_{0.85}Ca_{0.15})(Zr_{0.1}Ti_{0.9})O_3$ piezoelectric ceramics by at least 30 °C. Further investigations into the variation of piezoelectric properties with temperature and identification of the phase transitions are on-going.

Acknowledgment

This work was supported by the project "CEITEC - Central European Institute of Technology" (CZ.1.05/1.1.00/02.0068) from the European Regional Development Fund and by the Czech Science Foundation under grant number P108/13-09967S. The work was also financed from the SoMoPro II programme. The research leading to these results has acquired a financial grant from the People Programme (Marie Curie action) of the Seventh Framework Programme of EU according to the REA Grant Agreement No. 291782. The research is further co-financed by the South Moravian Region. It reflects only the views of the authors and that the Union is not liable for any use that may be made of the information contained therein.

References

[1] "EU-Directive 2002/95/EC: Restriction of the Use of Certain Hazardous Substances in Electrical and Electronic Equipment (RoHS)," Office Journal of the European Union, vol. 46, pp. 19-23, 2003.

[2] W. F. Liu and X. B. Ren, "Large Piezoelectric Effect in Pb-Free Ceramics," Phys. Rev. Lett., vol. 103, Dec 2009.

[3] B. C. Luo, D. Y. Wang, M. M. Duan, and S. Li, "Growth and characterization of lead-free piezoelectric BaZr0.2Ti0.8O3-Ba0.7Ca0.3TiO3 thin films on Si substrates," Appl. Surf. Sci., vol. 270, pp. 377-381, Apr 2013.

[4] W. F. Bai, B. Shen, F. Fu, and J. W. Zhai, "Dielectric, ferroelectric, and piezoelectric properties of textured BZT-BCT lead-free thick film by screen printing," Mater. Lett., vol. 83, pp. 20-22, Sep 2012.

[5] Y. Jiang, T. Thongchai, Y. Bai, C. Meggs, T. W. Button, A. Matousek, *et al.*, "Lead-free piezoelectric materials and composites for high frequency medical ultrasound transducer applications," in Ultrasonics Symposium (IUS), 2014 IEEE International, 2014, pp. 903-906.

[6] J. Rodel, W. Jo, K. T. P. Seifert, E. M. Anton, T. Granzow, and D. Damjanovic, "Perspective on the development of lead-free piezoceramics," J. Am. Ceram. Soc., vol. 92, pp. 1153-1177, 2009.

[7] S. Qiao, J. G. Wu, B. Wu, B. Y. Zhang, D. Q. Xiao, and J. G. Zhu, "Effect of Ba0.85Ca0.15Ti0.90Zr0.10O3 content on the microstructure and electrical properties of Bi-0.51(Na0.82K0.18) 0.50TiO3 ceramics," Ceram. Int., vol. 38, pp. 4845-4851, Aug 2012.

[8] Y. Bai, A. Matousek, P. Tofel, V. Bijalwan, B. Nan, H. Hughes, et al., "$(Ba,Ca)(Zr,Ti)O_3$ Lead-free Piezoelectric Ceramics – The Critical Role of Processing on Properties," J. Eur. Ceram. Soc., in press.